Return to Rodinia? Moderate to high palaeolatitude of the São Francisco/Congo craton at 920 Ma

D. A. D. EVANS[1]*, R. I. F. TRINDADE[2], E. L. CATELANI[2,3], M. S. D'AGRELLA-FILHO[2], L. M. HEAMAN[4], E. P. OLIVEIRA[5], U. SÖDERLUND[6], R. E. ERNST[7], A. V. SMIRNOV[8] & J. M. SALMINEN[9]

[1]*Department of Geology & Geophysics, Yale University, New Haven, CT 06520-8109, USA*

[2]*Instituto de Astronomia, Geofísica e Ciências Atmosféricas, Universidade de São Paulo, Rua do Matão, 1226, São Paulo, SP, 055080-090, Brazil*

[3]*Present Address: Octo Construções e Empreendimentos Ltda, Rua João Papaterra Limongi, 80 Butantã, São Paulo, SP-CEP, 05516-060, Brazil*

[4]*Department of Earth and Atmospheric Sciences, University of Alberta, Edmonton, Alberta, Canada T6G 2E3*

[5]*Department of Geology and Natural Resources, Institute of Geosciences, University of Campinas-UNICAMP, PO Box 6152, Campinas, 13083-970, Brazil*

[6]*Department of Geology, Lund University, Sölvegatan 12, SE 223 62 Lund, Sweden*

[7]*Department of Earth Sciences, Carleton University, Ottawa, Ontario, Canada K1S 5B6*

[8]*Department of Geological and Mining Engineering and Sciences, Michigan Technological University, 1400 Townsend Drive, Houghton, MI 49931, USA*

[9]*Department of Physics and Department of Geosciences and Geography, University of Helsinki, PO Box 64, Helsinki, 00014, Finland*

**Corresponding author (e-mail: david.evans@yale.edu)*

Abstract: Moderate to high palaeolatitudes recorded in mafic dykes, exposed along the coast of Bahia, Brazil, are partly responsible for some interpretations that the São Francisco/Congo craton was separate from the low-latitude Rodinia supercontinent at about 1050 Ma. We report new palaeomagnetic data that replicate the previous results. However, we obtain substantially younger U–Pb baddeleyite ages from five dykes previously thought to be 1.02–1.01 Ga according to the $^{40}Ar/^{39}Ar$ method. Specifically, the so-called 'A-normal' remanence direction from Salvador is dated at 924.2 $\pm$ 3.8 Ma, within error of the age for the 'C' remanence direction at 921.5 $\pm$ 4.3 Ma. An 'A-normal' dyke at Ilhéus is dated at 926.1 $\pm$ 4.6 Ma, and two 'A-normal' dykes at Olivença have indistinguishable ages with best estimate of emplacement at 918.2 $\pm$ 6.7 Ma. We attribute the palaeomagnetic variance of the 'A-normal' and 'C' directions to lack of averaging of geomagnetic palaeosecular variation in some regions. Our results render previous $^{40}Ar/^{39}Ar$ ages from the dykes suspect, leaving late Mesoproterozoic palaeolatitudes of the São Francisco/Congo craton unconstrained. The combined 'A-normal' palaeomagnetic pole from coastal Bahia places the São Francisco/Congo craton in moderate to high palaeolatitudes at *c.* 920 Ma, allowing various possible positions of that block within Rodinia.

Despite more than two decades of intense global research, the configuration of Neoproterozoic supercontinent Rodinia remains enigmatic. Following the first global synthesis by Hoffman (1991), most models include a central location for Laurentia, flanked by 'East' Gondwana-Land cratons along its proto-Cordilleran margin and 'West' Gondwana-Land cratons along its proto-Appalachian margin, and Siberia along its northern Canadian margin (e.g. Dalziel 1997). Early palaeomagnetic syntheses supported this kind of reconstruction (Powell *et al.* 1993; D'Agrella-Filho *et al.* 1998; Weil *et al.* 1998). The Hoffman-style models imply major reorganization of the Laurentian

From: Li, Z. X., Evans, D. A. D. & Murphy, J. B. (eds) 2016. *Supercontinent Cycles Through Earth History*. Geological Society, London, Special Publications, **424**, 167–190.
First published online May 28, 2015, http://doi.org/10.1144/SP424.1

connections following Rodinia breakup *en route* to the amalgamation of Gondwana-Land and ultimately Pangea, but entail relatively minor motions between each of the 'East' and 'West' Gondwana-Land cratonic groups through the same interval of time. In contrast, more recently acquired palaeomagnetic data (e.g. Wingate & Giddings 2000; Wingate *et al.* 2002) pose challenges to these models and have led to alternatives that question the existence of the supercontinent altogether (Meert & Torsvik 2003), exclude certain cratons (Pisarevsky *et al.* 2003), shorten the lifespan of Rodinia considerably (Li *et al.* 2008) or generate a radically different long-lived reconstruction (Evans 2009). Application of palaeomagnetic data to the problem requires not only a high reliability of the remanence directions, but also confidence in accurate dating of the rocks and their magnetic acquisitions.

One of the larger cratons in Meso-Neoproterozoic palaeogeography is the São Francisco (SF)/Congo craton, spanning eastern Brazil and formerly contiguous central Africa (Fig. 1). The SF/Congo craton is surrounded by latest Proterozoic to Cambrian orogens that welded together the supercontinent Gondwana-Land. Prior to that orogenic activity, a substantial proportion of the craton's margins were passive (Trompette 1994), established by rifting at *c.* 920 Ma (Araçuaí and West Congolese; Tack *et al.* 2001), *c.* 750 Ma (northern Damara and Lufilian; Hoffman & Halverson 2008; Key *et al.* 2001) and poorly dated but probably mid-Neoproterozoic (Oubanguide; Poidevin 2007). These rifted margins were created during the likely interval of Rodinia's breakup, and thus provide important conceptual impetus for including SF/Congo within the supercontinent. The interpretation of 1300–1000 Ma orogenic activity at the eastern margin of the SF/Congo craton (Kokonyangi *et al.* 2006; De Waele *et al.* 2009), during the nominal interval of Rodinia assembly, provides some further support for consideration of SF/Congo membership within the supercontinental landmass.

However, several recent studies have suggested that large regions of South America and central/southern Africa were absent from Rodinia. Kröner

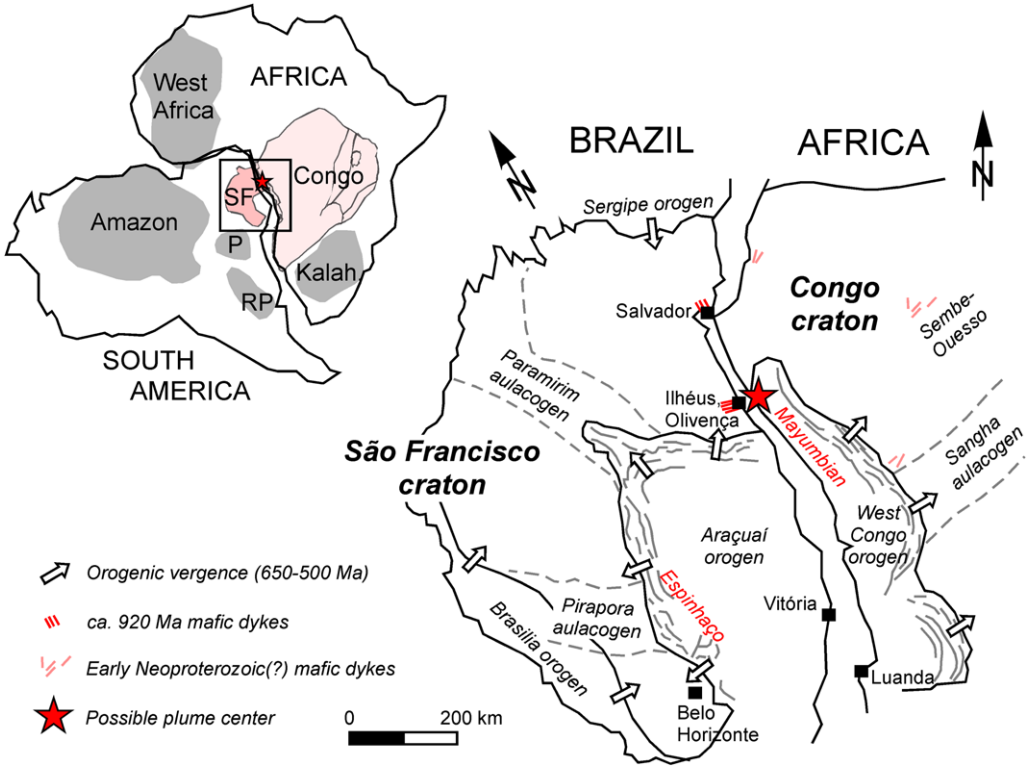

Fig. 1. Regional tectonic map of the São Francisco (SF)/Congo craton after reconstruction of the South Atlantic Ocean, with Phanerozoic cover removed (modified from Alkmim *et al.* 2006; schematic dyke trends from Correa-Gomes & Oliveira 2000). Inset, cratons of western Gondwana-Land: Kalah, Kalahari; P, Paranapanema; RP, Rio de la Plata; SF, São Francisco.

& Cordani (2003) based this argument on substantially different timing of orogeny and rifting among various regions such as Goiás, Mantiqueira, Borborema, Trans-Sahara and Madagascar, relative to the expected Rodinian ages of assembly and breakup as noted above. The 'Kibaran orogeny' of eastern SF/Congo could also represent mere arc–continent collisions (Johnson *et al.* 2005; De Waele *et al.* 2008) or largely thermal effects of intracratonic magmatism (Fernandez-Alonso *et al.* 2012), as opposed to continent–continent collisions. Independently, the interpretations of Cordani *et al.* (2003) and D'Agrella-Filho *et al.* (2004) have appealed to palaeomagnetic data from SF/Congo to substantiate a physical separation of the craton from others more plausibly connected to Rodinia. Namely, high palaeolatitudes for SF/Congo during the interval 1080–1010 Ma were contrasted with the low-latitude positions of Laurentia, Siberia, Australia and Kalahari through those times.

The SF/Congo palaeomagnetic poles generating the high palaeolatitudes discussed above come from mafic dyke swarms in coastal Bahia, Brazil: Salvador, Ilhéus, Itaju do Colônia and Olivença (Figs 1 & 2). As described in previous studies (e.g. D'Agrella-Filho *et al.* 1990, 2004), the dykes are composed of diabase, containing primary subophitic igneous textures and essentially unmetamorphosed

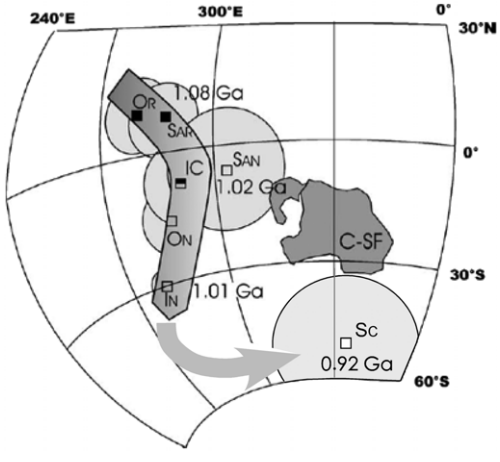

Fig. 2. Traditional representation of the palaeomagnetic apparent polar wander path from Bahia mafic dykes, in present South American coordinates. Ages are $^{40}Ar/^{39}Ar$ determinations (Renne *et al.*1990; D'Agrella-Filho *et al.* 2004) discussed in text. C-SF, Congo/São Francisco craton; IC, Itaju do Colônia; I, Ilhéus; O, Olivença; S, Salvador (with 'A' or 'C' subscripts); N, 'normal' (upward remanence inclination); R, 'reversed' (downward remanence inclination). Modified from D'Agrella-Filho *et al.* 2004.

aside from deuteric alteration within the interiors of some of the coarser-grained intrusions. Early palaeomagnetic (D'Agrella-Filho *et al.* 1990) and $^{40}Ar/^{39}Ar$ (Renne *et al.* 1990) studies on these dyke swarms generated a series of poles defining the 1080–1010 Ma apparent polar wander (APW) path for the SF/Congo craton: the Olivença 'reversed' polarity pole at 1078 ± 18 Ma, the Ilhéus 'normal' polarity pole at 1012 ± 24 Ma and undated intermediate poles from Itaju do Colônia (dual polarity) and Olivença ('normal'). In the Southern Hemisphere, the convention is to refer to upward north-seeking directions as 'normal' polarity and downward north-seeking directions as 'reversed' polarity, despite the unknown absolute polarity sense owing to incompleteness of APW paths backward from Phanerozoic into Precambrian time. We follow that convention herein.

The Bahia palaeomagnetic dataset was further substantiated by D'Agrella-Filho *et al.* (2004), on dykes from Salvador, including additional $^{40}Ar/^{39}Ar$ ages of *c.* 1030–1000 Ma and two positive baked-contact tests on 'reversed' polarity dykes into Palaeoproterozoic host rocks. An attempted baked-contact test on the 'normal' polarity dyke at the 'Meridian' locality was judged by the authors to be inconclusive. In addition to these poles, all given the code letter 'A', results were reported from an undated group of dykes in the Valéria quarry (code letter 'B') and three dykes exposed along the Salvador beaches with a southerly downward characteristic remanence direction (code letter 'C') that was associated with a preliminary U–Pb baddeleyite age of *c.* 924 Ma (Heaman 1991, abstract only). Note that the letter designations (A, B, C) refer only to characteristic remanence site-mean directions, not vector components within individual samples. The APW path derived from standard interpretation of these results is summarized in Figure 2.

The present study was motivated towards obtaining additional precise U–Pb ages from the various Bahia dyke swarms, notably dykes carrying the 'A' and 'C' remanence directions, in order to test the validity of the $^{40}Ar/^{39}Ar$ ages, to refine the APW path for SF/Congo, and ultimately to test whether that craton could have been part of Rodinia.

Methods

In order to determine which palaeomagnetic remanence directions would correspond with our new U–Pb ages, it was necessary to identify dykes in the field corresponding to the published poles. Because much of the previously published work (D'Agrella-Filho *et al.* 1990, 2004) derived from block samples collected prior to the availability of

GPS technology, it was necessary for us to collect our palaeomagnetic samples from as many dykes as possible for complete coverage of the three coastal field areas: Salvador, Ilhéus and Olivença. The sampling strategy was designed for verifying the existing published data rather than generating entirely new data, so only two cores were drilled in each dyke. Nonetheless, the cores were long enough to facilitate both alternating-field (AF) and thermal demagnetization procedures on sister specimens; this allowed for typically four estimates of the palaeomagnetic remanence directions at each site, and most samples were very stable to both AF and thermal demagnetization, yielding identical results from both methods. Thermal demagnetization was carried out in nitrogen-atmosphere ASC-Scientific magnetically shielded furnaces, and high-level AF demagnetization utilized a Molspin tumbler apparatus with self-reversing spin mechanism. Measurements were made on a 2G (now WSGI) cryogenic magnetometer with an automated sample-changing system (Kirschvink *et al.* 2008) at Yale University, except for the baked-contact tests, which were measured with an AGICO JR6 spinner magnetometer at the Universidade de São Paulo. Vector components were isolated using principal component analysis (Kirschvink 1980) and analysed with Fisher (1953) statistics, giving unit weight to each specimen to compute a site mean. Directional data were complemented by rock-magnetic data: magnetic hysteresis, using a model 2900 Princeton Measurement Corporation Alternating Gradient Field Magnetometer, and thermomagnetic analyses, using an AGICO KLY-4S magnetic susceptibility meter equipped with a high-temperature furnace and a cryostat.

Geochronologic samples for this study were collected during four excursions and by four different researchers: SAL2-90 and SAL5-90 were collected by T. Onstott (Princeton) in 1990; LH91-13 was collected by L. M. Heaman in 1991; OL4 and OL26 were collected by D. Evans, M. D'Agrella-Filho, and R. Trindade in 2006; and OLIV-3 was collected by E. Oliveira in 2009. Sample processing and U–Pb analyses were conducted at three laboratories denoted with the following abbreviations in Table 1: ROM – Royal Ontario Museum (now at the University of Toronto); UofA – University of Alberta (Edmonton); and LIG – Laboratory for Isotope Geology at the Swedish Museum of Natural History (Stockholm). Baddeleyite extraction was accomplished using slightly different techniques over the duration of this study; samples processed at the Royal Ontario Museum were pulverized in a jaw crusher and Bico disc mill, heavy mineral concentrate obtained using a Wilfley table and final baddeleyite concentrate using standard magnetic (Frantz Isodynamic Separator) and density (heavy liquids) techniques. For samples collected since 2009, smaller hand samples were cut into slabs and pulverized using a tungsten-carbide puck mill (UofA), and baddeleyite concentration followed the Wilfley table procedure outlined by Söderlund & Johansson (2002).

In most of the samples, the baddeleyite crystals were minuscule (<20 μm in longest dimension) and were hand selected, washed in warm 4 N HNO_3 for 1 h, and cleaned by repeat rinses in Millipore H_2O and acetone. The selected grains were loaded into TFE Krogh-type dissolution vessels together with a measured amount of $^{205}Pb/^{235}U$ ($^{205}Pb/^{233-236}U$ at LIG) tracer solution and a mixture of HF/HNO_3 (10:1), placed in an oven at 220 °C for at least 36 h, evaporated to dryness and converted to a chloride form by placing in the oven again overnight with 3.1 N HCl. Uranium and lead were purified using anion exchange chromatography for fractions weighing >1 μg (Heaman & Machado 1992; French & Heaman 2010) The isotopic composition of U and Pb were determined using a VG354 (ROM and UofA) and a Finnigan Triton (LIG) thermal ionization mass spectrometer operating in single collector peak hopping mode. Typical in-run 1 σ standard deviation measurement errors were $<0.5\%$ for $^{207}Pb/^{206}Pb$ and $^{238}U/^{235}U$. All isotopic data were corrected for mass discrimination, detector bias, spike contribution, blank (ROM: 5 pg Pb, 1 pg U; UofA: 1.0 pg Pb, 0.5 pg U; LIG: 0.6 pg Pb, 0.2 pg U) and initial common Pb (Stacey & Kramers 1975). The total uncertainty for each analysis was determined by numerically propagating all known sources of error. All age calculations and plots were prepared using the Isoplot software of Ludwig (2003) with the ^{238}U and ^{235}U decay constants and $^{238}U/^{235}U$ value reported by Jaffey *et al.* (1971).

Results: U–Pb geochronology

The U–Pb results for 11 baddeleyite fractions selected from four dyke samples are compiled in Table 1. The U–Pb results are presented in Figure 3. Two dyke samples were investigated from the Salvador area, informally known as the Meridian and Ondina dykes. Baddeleyite from two samples of the Meridian dyke (SAL2-90 and LH91-13) are less than 2% discordant and have $^{207}Pb/^{206}Pb$ dates that vary between 919.3 and 924.7 Ma, but overlap within analytical uncertainty (Fig. 3a). The weighted mean $^{207}Pb/^{206}Pb$ date using all three analyses is 924.2 ± 3.8 Ma (MSWD $= 0.3$) and is considered to be a good constraint for the emplacement age of this dyke.

The U–Pb results for three baddeleyite fractions from the Ondina dyke (SAL5-90) are displayed

Table 1. *U–Pb ID thermal ionization mass spectrometer baddeleyite results for Neoproterozoic mafic dykes in coastal Bahia, Brazil*

	Description (with analysis no.)	Weight (μg)	U (ppm)	Th (ppm)	Pb (ppm)	Th/U Th/U	TCPb (pg)	$^{206}Pb/^{204}Pb$	$^{206}Pb/^{238}U$	1σ error	$^{207}Pb/^{235}U$	1σ error	$^{207}Pb/^{206}Pb$	1σ error	ρ	Model ages (Ma)			1σ error	$^{207}Pb/^{206}Pb$	1σ error	%Disc
																$^{206}Pb/^{238}U$	1σ error	$^{207}Pb/^{235}U$				
	Salvador dykes																					
	Meridian Dyke (LH91-13 and SAL2-90)																					
1	LH91-13; best fragments (67) ROM	10	221	19	33	0.08	13	1606	0.15274	0.00019	1.4715	0.0021	0.06988	0.00007	0.73	916.3	1	918.8	0.9	924.7	2	1
2	SAL2-90; M3+5 2nd best (5)* UofA	1	250	50	41	0.2	6	427	0.15044	0.00028	1.4457	0.0061	0.06969	0.00027	0.401	903.5	1.6	908.1	2.5	919.3	7.9	1.8
3	SAL2-90; M3+5 best (5)* UofA	1	169	10	28	0.06	5	351	0.15116	0.00057	1.4535	0.0089	0.06974	0.00038	0.476	907.5	3.2	911.3	3.7	920.6	11.2	1.5
	Ondina Dyke (SAL5-90-1)																					
1	Light brown fragments, 1 + 3 + 5M (34) ROM	4	227	25	35	0.11	13	660	0.14999	0.00028	1.4437	0.0069	0.06981	0.0003	0.477	900.9	1.6	907.3	2.9	922.8	8.7	2.5
2	Light brown fragments, 1 + 3 + 5M (58) ROM	6	269	30	40	0.11	10	1560	0.15255	0.00017	1.4674	0.0022	0.06976	0.00008	0.694	915.3	0.9	917.1	0.9	921.4	2.3	0.7
3	Brown fragments with black incl (4) UofA	1	185	27	40	0.15	15	139	0.15277	0.00053	1.4713	0.0233	0.06985	0.00106	0.302	916.4	2.9	918.7	9.5	924	30.8	0.9
	Ilhéus (Pernambuco) Dyke																					
	OLIV-3																					
1	Light brown fragments (3) LIG	n.m.	n.m.	n.m.	n.m.	0.44	0.8	320	0.15141	0.0017	1.4589	0.0172	0.06988	0.00033	0.892	908.8	11.5	913.5	8.5	924.9	9.6	1.6
2	Light brown fragments (7) LIG	n.m.	n.m.	n.m.	n.m.	0.36	0.6	975	0.15198	0.00058	1.466	0.006	0.06996	0.00012	0.904	912.1	4.3	916.5	3	927.1	3.6	1.6
3	Light brown fragments (2) LIG	n.m.	n.m.	n.m.	n.m.	0.28	0.6	950	0.15141	0.00045	1.4589	0.0047	0.06988	0.0001	0.892	908.8	3.1	913.5	2.5	924.9	3	1.7
	Olivença Dykes																					
	OL4																					
1	Incl in quartz (4)* UofA	0.5	274	62	122	0.23	43	47	0.15018	0.00174	1.4694	0.0557	0.07096	0.00279	0.035	902	9.7	917.9	22.7	956.3	78.3	6.1
2	Tiny brown fragment (1)* UofA	0.2	174	17	42	0.1	4	92	0.15279	0.00133	1.4728	0.0364	0.06991	0.00161	0.37	916.6	7.4	919.3	14.9	925.7	46.5	1.1
3	Tiny brown fragment (1)* UofA	0.2	130	21	39	0.16	5	65	0.15028	0.00188	1.5346	0.0518	0.07406	0.00235	0.346	902.5	10.5	944.3	20.5	1043.1	62.6	14.4
	OL26																					
1	Tiny brown fragments, NM0.6A (4)* UofA	0.5	183	18	39	0.1	7	137	0.15361	0.00062	1.4811	0.0174	0.06993	0.00079	0.273	921.2	3.5	922.7	7.1	926.3	23.1	0.6
2	Tiny brown fragments, NM0.6A (4)* UofA	0.4	107	11	30	0.1	7	76	0.15104	0.00123	1.4544	0.0357	0.06984	0.00166	0.264	906.8	6.9	911.7	14.7	923.6	48.1	2

Notes: Numbers in parentheses correspond to the number of crystals analysed. * Weights estimated. Incl, Mineral inclusions; ROM, analyses conducted at the Royal Ontario Museum; UofA, analyses conducted at the University of Alberta; LIG, analyses conducted at the Laboratory of Isotope Geology, Stockholm.
Atomic ratios corrected for blank, fractionation and initial common Pb (Stacey & Kramers 1975).
Th concentration estimated from the amount of ^{208}Pb present in the analysis and the $^{207}Pb/^{206}Pb$ age.
TCPb refers to the total amount of common lead present in the analyses in picograms. ρ refers to the correlation coefficient between $^{206}Pb/^{238}U$ and $^{207}Pb/^{235}U$ ratios. %Disc refers to the amount of discordance along a reference line to zero age.
All errors in this table are reported at 1σ (0.09402 ± 2 means 0.09402 ± 0.00002).
n.m., Not measured.

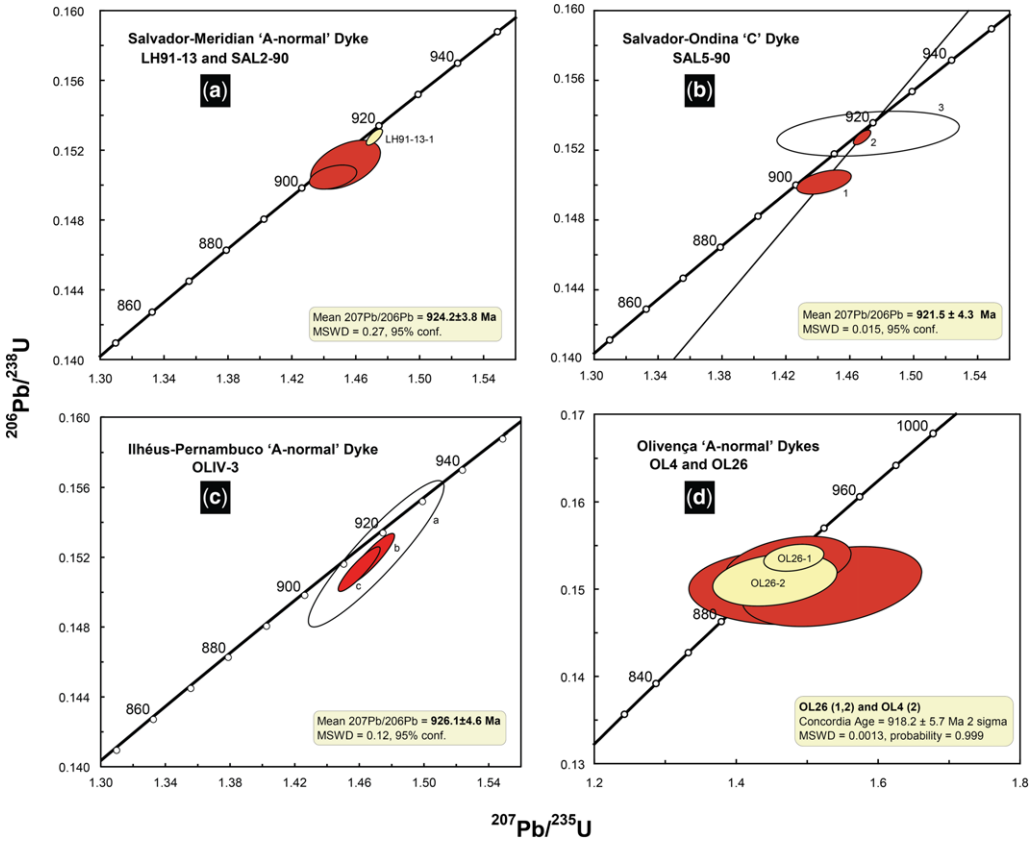

Fig. 3. Wetherill concordia plots of U–Pb baddeleyite data for Bahia diabase dykes. (**a**) U–Pb baddeleyite results for two samples of the Meridian dyke, Salvador. (**b**) U–Pb baddeleyite results for the Ondina dyke, Salvador. (**c**) U–Pb baddeleyite results for two Olivença dykes (OL4 and OL26). and (**d**) U–Pb baddeleyite results for the Pernambuco dyke, Ilhéus.

on a concordia plot in Figure 3b. Fractions 2 and 3 are concordant, that is, they plot within error of the concordia curve and are $<1\%$ discordant. All three analyses have identical $^{207}Pb/^{206}Pb$ dates within analytical uncertainty and define a weighted average $^{207}Pb/^{206}Pb$ date of 921.5 $\pm$ 4.3 Ma (MSWD = 0.02). This date is constrained primarily by the most precise analysis #2.

The baddeleyite fractions of the OLIV-3 sample, from the widest dyke at Pernambuco Hill in the municipality of Ilhéus, overlap and plot immediately below the concordia curve, with about 1.5% discordance (Fig. 3c). All three analyses have identical $^{207}Pb/^{206}Pb$ dates within analytical uncertainty and define a weighted average $^{207}Pb/^{206}Pb$ date of 926.1 $\pm$ 4.6 Ma (MSWD = 0.12).

A tiny amount of minuscule baddeleyite (<15 crystals and fragments) was recovered from two dyke samples (OL4 and OL26) in the Olivença area. The total amount of radiogenic Pb in these analyses was very small (<30 pg) and the corresponding uncertainties are much larger than the results obtained from the Meridian and Ondina dyke samples above. All five analyses are displayed on a concordia plot in Figure 3d, and the two analyses from sample OL26 are shown as yellow ellipses. All five analyses overlap the concordia curve within error, and the three most precise analyses (OL4-2, OL26-1 and OL26-2) yield a concordia age of 918.2 $\pm$ 5.7 Ma, interpreted to be the best estimate for the emplacement age of these two dykes.

Overall, the U–Pb age results for the five dyke samples from Salvador, Ilhéus and Olivença are indistinguishable within analytical uncertainty. As will be discussed below, all of these ages correspond to either the 'A-normal' or 'C' palaeomagnetic remanence directions, with implications for interpretations of the Bahia dykes' palaeomagnetic poles and Rodinia reconstructions.

Results: rock magnetism and palaeomagnetism

Magnetic hysteresis loop parameters (coercivity, H_c; coercivity of remanence, H_{cr}; saturation remanence, M_{rs}; and saturation magnetization, M_s) indicate the presence of a magnetic mineral phase with intermediate-to-high coercivity (Fig. 4a, c, e). The M_{rs}/M_s and H_{cr}/H_c ratios suggest a pseudo-single domain magnetic carrier in our samples (Day *et al.* 1977). Temperature dependence of low-field magnetic susceptibility, $\kappa(T)$, was measured from −192 to *c.* 700 °C (in argon) followed by cooling back to room temperature. The thermomagnetic curves from all of the samples are nearly reversible, revealing the presence of a single magnetic phase with a Curie temperature between 575 and 585 °C (Fig. 4b, d, f), consistent with magnetite and/or low-Ti titanomagnetite as a magnetic carrier. A characteristic peak observed at −153 °C, associated with the Verwey transition (Verwey 1939) indicates that the magnetite is nearly stoichiometric. Overall, the results of our rock-magnetic analyses are consistent with the rock magnetic and microscopy data presented by D'Agrella-Filho *et al.* (1990, 2004).

Palaeomagnetic results are listed in Table 2, and representative demagnetization behaviours are illustrated in Figures 5, 7 and 8. Site mean directions from each locality are combined with site means from D'Agrella-Filho *et al.* (1990, 2004), even though we recognize that some of the same dykes have been analysed both by us and by the previous studies. This is justified by the fact that measurements come from different laboratory demagnetization experiments and are thus independent, and also because the number of doubly analysed sites is estimated to be small relative to the entire number of sites contributing to the grand mean palaeomagnetic pole. Among all datasets, only site-means derived from more than two samples and with Fisher (1953) a_{95} values less than 20° are included in the overall mean calculations.

Salvador

Along the beaches of Salvador city (Fig. 5), four dykes were sampled (SA16, 17, 19 and 22). The site-numbering system was intended to mimic that of D'Agrella Filho *et al.* (2004), and despite the lack of GPS coordinates from the earlier study, we are confident that all except SA19 do indeed correspond to the site numbers of the earlier study – based on the outcrop map in the unpublished PhD thesis of M.S. D'Agrella-Filho (1992), as well as our palaeomagnetic results. Our site SA19 is located at the base of the breakwater wall, almost directly north of the Farol da Barra, from a NNW-striking, 2 m-wide dyke with numerous previous drill holes from a magnetic anisotropy study (Raposo & Berquó 2008). This site showed a scattered characteristic remanent magnetization (ChRM) directed West-Up, which could represent either an extreme outlier of the A-normal direction or the antipode of the B direction. Lacking unambiguous grouping with one of the known Bahia dyke ChRM directions, this result is not discussed further herein. The other three dykes from Salvador were collected at two localities. At the small 'Ondina' cove, the north-striking, 13 m-wide dyke (SA22), bearing the new U–Pb baddeleyite age of 922 ± 4 Ma, is the same intrusion as that referred to by Heaman (1991). After removal of a low-coercivity overprint, this dyke exhibits the C remanence direction (Table 2, Fig. 5), as earlier determined from the same site by D'Agrella-Filho *et al.* (2004). Unlike the vast majority of samples in this study, AF demagnetization did not isolate the ChRM well at this site. At the 'Meridian' locality directly below the Ibis hotel, two dykes (SA16, SA17) carry opposite remanence polarities. The 1.5 m-wide, WNW-striking dyke (SA16), which is older, has the A-reversed direction that was verified by a positive baked-contact test into basement granulites by D'Agrella-Filho *et al.* (2004). The younger, 20–25 m-wide, NNW-striking dyke (SA17) has the A-normal direction and bears the new U–Pb baddeleyite age of 924 ± 4 Ma, reported above. Although the baked-contact test of this large dyke into Palaeoproterozoic basement rocks was judged by D'Agrella-Filho *et al.* (2004) to be inconclusive, we note that the presence of the A-reversed direction at SA16, merely tens of metres away in similar mafic lithology, suggests that the locality has not been magnetically overprinted since intrusion of the younger, larger SA17 dyke (i.e. the SA17 A-normal remanence is suggested to be primary). The intersection of these dykes is located within the storm surge zone, and heavy weather conditions (over three separate visits) unfortunately prevented us from sampling a complete baked-contact test between the two dykes, of opposite polarities, at the locality.

In summary of the Salvador results (Fig. 6), we confirm that our new U–Pb ages correspond to both the C (Ondina, 922 ± 4 Ma) and A-normal (Meridian, 924 ± 4 Ma) remanence directions, which are both within error of the palaeomagnetic data reported for those same sites by D'Agrella-Filho *et al.* (2004). We filter the data to accept only those sites having three or more specimens contribute to the mean direction (Table 2); thereafter, none of the mean directions (A-normal, A-reversed, C) contain enough sites to guarantee adequate time-averaging of the geomagnetic field. Another problem is that the A-normal and A-reversed means, whether quality-filtered or not,

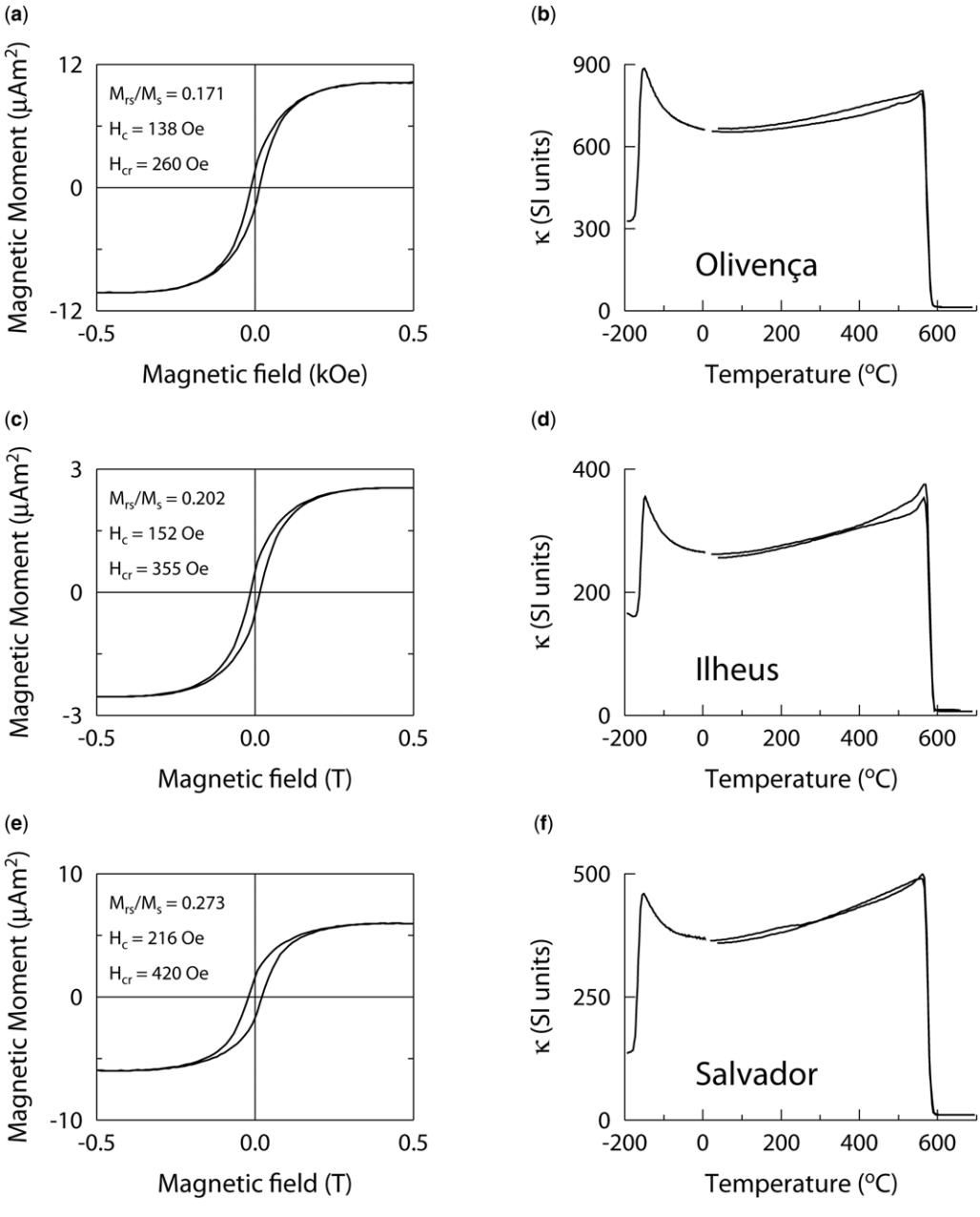

Fig. 4. (**a**, **c**, **e**) Typical magnetic hysteresis loops after paramagnetic slope correction measured from Olivença (a), Ilhéus (c) and Salvador (e) dykes. Abbreviations: H_c, coercivity; H_{cr}, coercivity of remanence; M_{rs}, saturation remanence; M_s, saturation magnetization. (**b**, **d**, **f**) Typical low-field thermomagnetic curves (κ(T)) measured in argon from −192 to 700 °C from Olivença (b), Ilhéus (d) and Salvador (f) dykes.

differ from anti-parallelism at greater than 95% confidence level (McFadden & McElhinny 1990). Therefore, although we calculate a two-polarity palaeomagnetic pole for the Salvador 'A' directions (Table 2), we prefer to combine data from the Salvador region with the other studied areas before making tectonic interpretations. Although D'Agrella-Filho *et al.* (2004) corrected for an

Table 2. *Palaeomagnetic data from Proterozoic dykes of coastal Bahia, Brazil*

Site abbreviation	Comp.	Latitude (°S)	Longitude (°W)	*w* (m)	Strike/dip	*n*/*N*	GDec	GInc	*k*	a_{95}	Plat (N)	Plong (E)	Reference/mean stats	U–Pb age (Ma)
Salvador														
1	C	12.83	38.34	20	005/?	10/?	178.8	59.6	–	12.4	−62.2	323.6	D'AF + 04	
8	Ar	12.96	38.35	2	315/?	5/?	295.9	57.1	195	5.5	11.4	275.3	D'AF + 04	
9	Ar	12.96	38.36	1.5	315/?	4/?	286.9	59.6	340	4.9	03.9	274.8	D'AF + 04	
16	(Ar)	13.02	38.48			3/?	293.2	71.6	68	15.0	01.4	290.9*	D'AF + 04	
SA16	(Ar)	13.0159	38.4849	1.5	295/75 E	2/2	302.8	68.7	708	9.4	08.5	290.0	This study	
16 comb.	Ar					5/?	297.4	70.5	120	7.0	04.3	290.5	This study	
17	(An)	13.02	38.48			6/?	086.8	−80.5	206	4.7	−13.3	302.5*	D'AF + 04	
SA17	(An)	13.0158	38.4847	20	330/90	4/4	142.1	−77.1	108	8.9	06.6	306.6*	This study	
17 comb.	An					10/?	112.9	−80.4	96	5.0	−05.3	304.3*	This study	924.2 ± 3.8
18	An	13	38.53	0.6	323/?	3/?	136.8	−64.6	1149	3.6	19.0	291.6*	D'AF + 04	
19	An	13	38.53	3.5	339/?	3/?	149.7	−65.0	73	14.5	24.2	299.3*	D'AF + 04	
SA19	(An)	13.0081	38.5325	2	325/70 E	4/4	268.5	−74.1	26	18.5	−10.5	351.7*	This study	
22	(C)	13.01	38.51			4/?	167.2	61.4	49	13.2	−58.4	339.7	D'AF + 04	
SA22	(C)	13.0107	38.5147	13	350/73 E	5/8	173.2	67.7	108	7.4	−52.0	328.5	This study	
22 comb.	C					9/?	170.2	64.9	71	6.2	−55.1	333.2	This study	921.5 ± 4.3
23	An	13.01	38.53	2	015/?	3/?	082.5	−83.5	224	8.2	−14.3	308.3*	D'AF + 04	
Mean	An		*Salvador only*			4†	133.3	−74.4	46	13.7	06.0	301.0*	$K = 16.7, A_{95} = 23.2°$	
Mean	Ar		*Salvador only*			3†	293.0	62.5	114	11.6	06.7	280.0	$K = 65.9, A_{95} = 15.3°$	
Mean	An + Ar		*Salvador only*			7†	301.8	69.5	45	9.1	06.4	291.9	$K = 18.7, A_{95} = 14.3°$	
Mean	C		*Salvador only*			2†	174.9	62.3	299	14.5	−58.9	328.9	$K = 164.5, A_{95} = 19.6°$	
Ilhéus														
IL1	An	14.8077	39.0238	12	245/90	7/8	064.6	−58.1	198	4.3	−28.9	267.4*	This study	926.1 ± 4.6
IL2	An	14.8061	39.0239	10	245/77 N	4/4	055.9	−71.6	183	6.8	−30.7	289.0*	This study	
IL3	An	14.8059	39.0241	10	230/undul.	4/4	046.0	−64.8	1353	2.5	−40.3	280.8*	This study	
IL4	An	14.8055	39.0242	0.9	240/65 N	4/4	044.6	−61.3	378	4.7	−42.9	276.0*	This study	
IL5	An	14.8054	39.0243	1.5	240/90	4/4	044.8	−60.6	1031	2.9	−43.1	274.8*	This study	
IL6	An	14.8052	39.0245	7	248/90	4/4	048.4	−68.9	361	4.8	−36.5	286.4*	This study	
IL7	An	14.8051	39.0253	2	250/72 N	4/4	057.4	−63.4	467	4.3	−33.3	275.5*	This study	
IL8	An	14.805	39.0255	0.6	243/77 N	4/4	072.9	−58.8	111	8.8	−22.4	268.1*	This study	
IL9	An	14.805	39.0255	0.7	230/90	4/4	062.1	−61.0	151	7.5	−30.5	271.4*	This study	
IL11	An	14.8514	39.0407	4	230/undul.	4/4	042.4	−73.2	442	4.4	−29.9	274.9*	This study	
IL12	An	14.8513	39.0407	3.5	240/undul.	4/4	062.3	−63.5	996	2.9	−34.3	277.4*	This study	
52	An	14.81	39.02	10	280	4/4	065.6	−60.6	76	10.6	−27.9	270.5*	D'AF + 90	
53	An	14.81	39.02	3	270	3/3	045.4	−65.2	813	4.3	−40.3	281.6*	D'AF + 90	
54	An	14.81	39.02	8	260	3/3	042.3	−70.8	53	17.0	−38.1	291.6*	D'AF + 90	
55	An	14.81	39.02	1	260	3/3	053.3	−64.8	1371	3.3	−35.5	278.5*	D'AF + 90	
56	An	14.81	39.02	2	260	3/3	051.0	−65.6	84	13.5	−36.6	280.3*	D'AF + 90	
57	An	14.81	39.02	6	260	3/3	049.1	−65.4	211	8.4	−37.9	280.7*	D'AF + 90	
58	An	14.81	39.02	0.5	255	3/3	063.5	−63.5	293	7.2	−29.0	274.8*	D'AF + 90	
59	An	14.81	39.02	2	270	3/3	059.9	−60.9	99	12.4	−32.0	271.4*	D'AF + 90	
60	An	14.81	39.02	1.5	260	4/4	054.4	−64.2	99	9.2	−35.0	277.3*	D'AF + 90	
62	An	14.8	39.03	4	270	3/3	073.8	−70.2	775	4.4	−21.3	283.9*	D'AF + 90	
63	An	14.8	39.03	1	285	3/3	060.4	−71.4	514	5.4	−28.5	287.4*	D'AF + 90	
64	An	14.79	39.03	1.5	260	3/3	079.5	−73.2	225	8.2	−18.0	288.7*	D'AF + 90	
65	An	14.79	39.03	1.5	260	3/3	073.3	−66.5	1080	3.7	−21.9	278.2*	D'AF + 90	
66	An	14.79	39.03	4	230	3/3	058.2	−63.9	231	8.1	−32.5	276.0*	D'AF + 90	

(*Continued*)

Table 2. *Continued*

Site abbreviation	Comp.	Latitude (°S)	Longitude (°W)	*w* (m)	Strike/dip	*n*/*N*	GDec	GInc	*k*	a_{95}	Plat (N)	Plong (E)	Reference/mean stats	U–Pb age (Ma)
68	An	14.78	39.1	?	?	3/3	065.0	−68.0	1512	3.1	−27.0	281.1*	D'AF + 90	
69	An	14.78	39.1	?	?	3/3	085.6	−71.7	91	13.0	−14.7	286.3*	D'AF + 90	
Mean	An		*Ilhéus only*			27†	058.4	−66.0	161	2.2	−31.8	279.6*	$K = 71.3$, $A_{95} = 3.3°$	
Olivença														
OL1	An	14.9582	39.0051	10	045	4/4	070.4	−60.6	262	5.7	−24.4	270.3*	This study	
OL2	(An)	14.9567	39.0067	>2	060	2/4	051.2	−53.6	67	31.1	−40.2	263.3*	This study	
OL3	An	14.9551	39.0074	0.3	050	6/6	070.2	−71.1	497	3.0	−23.4	285.6*	This study	
OL4	An	14.9529	39.0076	12	035	8/8	077.4	−59.8	146	4.6	−19.1	269.4*	This study	*c.* 920
OL5	(An)	14.9526	39.0074	6	075	4/4	077.0	−58.4	15	24.2	−19.4	267.7*	This study	
OL6	Ar	14.9517	39.0074	>2	070	4/4	327.3	54.9	38	15.0	30.9	290.1	This study	
OL7	(Ar)	14.951	39.0075	3.5	040	4/4	321.7	60.4	16	23.4	23.5	290.5	This study	
OL8	(Ar)	14.951	39.0075	0.4	070	2/4	295.0	58.1	41	40.0	09.0	275.3	This study	
OL9	Ar	14.9507	39.0077	2	060	4/4	268.5	56.1	70	11.1	−10.0	266.5	This study	
OL10	Ar	14.9503	39.0081	1.2	075	4/4	333.8	76.0	47	13.5	09.0	275.3	This study	
OL11	(Ar)	14.9482	39.0087	10	060	2/4	307.0	46.1	19	61.4	23.4	270.5	This study	
OL12	Ar	14.9477	39.0086	3.3	065	3/4	274.4	56.9	94	12.8	−05.6	268.3	This study	
OL13	(Ar?)	14.9471	39.0088	>2	080	4/4	290.7	26.2	10	30.2	15.7	250.4	This study	
OL14	(An)	14.9437	39.0108	40	060	2/4	099.7	−65.1	480	11.4	−04.5	278.7*	This study	
OL15	An	14.9321	39.0154	5	040	4/4	090.4	−77.0	157	7.4	−13.4	295.5*	This study	
OL16	An	14.9312	39.0155	24	055	4/4	098.1	−75.2	520	4.0	−09.5	293.0*	This study	
OL17	An	14.9308	39.016	6	075	4/4	029.5	−70.1	112	8.7	−44.6	297.1*	This study	
OL18	(Ar?)	14.9296	39.0165	6	080	2/4	323.5	49.6	34	44.1	32.6	283.5	This study	
OL19	(??)	14.9274	39.0171	>2	055	4/4	273.5	−47.0	46	13.6	10.0	204.3	This study	
OL20	–	14.9272	39.0171	>2	085	0/4	–	–	–	–	–	–	This study	
OL21	(??)	14.9268	39.0173	1.3	090	4/4	316.3	−59.1	12	27.5	44.5	189.1	This study	
OL22	An	14.9267	39.0174	1.8	060	4/4	107.9	−68.6	378	4.7	−01.1	285.0*	This study	
OL23	An	14.9262	39.0176	7	075	4/4	085.6	−71.0	313	5.2	−14.7	285.2*	This study	
OL24	–	14.9246	39.0181	>2	080	0/4	–	–	–	–	–	–	This study	
OL25	–	14.924	39.0182	>2	060	0/4	–	–	–	–	–	–	This study	
OL26	An	14.9228	39.0185	>5	ENE?	4/4	100.9	−56.3	104	9.1	−00.5	269.2*	This study	*c.* 920
4	An	14.99	39	1	060	3/3	140.1	−73.8	449	5.8	08.6	302.0*	D'AF + 90	
6	An	14.98	39	20	080	3/3	129.1	−58.6	266	7.7	17.9	281.9*	D'AF + 90	
11	An	14.95	39.01	20	070	3/3	064.9	−64.1	541	5.3	−28.0	285.3*	D'AF + 90	
13	Ar	14.95	39.01	1.2	098	3/3	312.9	56.0	64	15.4	21.9	281.5	D'AF + 90	
18b	Ar	14.95	39.01	?	?	4/4	292.6	51.8	28	17.6	10.1	268.7	D'AF + 90	
22	Ar	14.95	39.01	0.8	080	3/3	299.3	65.1	79	13.9	07.6	284.2	D'AF + 90	
23	Ar	14.95	39.01	15	085	3/3	314.4	63.2	86	13.4	17.4	288.8	D'AF + 90	

24b	Ar	14.95	39.01	?	?	5/5	294.7	61.5	183	5.6	07.0	278.6	D'AF + 90
26	Ar	14.94	39.01	1.5	110	3/3	321.7	61.6	268	7.5	22.4	291.4	D'AF + 90
28	An	14.94	39.01	2	060	3/3	054.9	−67.4	146	10.2	−33.6	282.0*	D'AF + 90
30	An	14.93	39.02	3.5	090	3/3	093.3	−74.2	270	7.5	−11.3	290.8*	D'AF + 90
31	An	14.93	39.02	1	075	3/3	072.5	−69.5	458	5.7	−22.3	282.8*	D'AF + 90
32	An	14.93	39.02	2	080	3/3	089.5	−71.9	172	9.4	−12.7	286.8*	D'AF + 90
34	An	14.92	39.02	15	055	3/3	074.2	−76.6	64	15.4	−20.2	294.8*	D'AF + 90
35	An	14.92	39.02	1	080	3/3	056.9	−70.6	3873	1.9	−30.9	286.7*	D'AF + 90
37	An	14.92	39.02	0.6	095	4/4	026.7	−77.3	103	9.0	−22.2	296.6*	D'AF + 90
39	An	14.91	39.02	2	065	3/3	195.9	−80.7	64	15.6	02.4	325.8*	D'AF + 90
40	An	14.91	39.02	3	080	3/3	100.3	−72.2	500	5.5	−07.1	288.6*	D'AF + 90
41	An	14.91	39.02	6	080	3/3	094.9	−69.7	610	4.9	−09.1	284.1*	D'AF + 90
42	An	14.91	39.02	1	090	3/3	090.2	−73.0	254	7.7	−12.6	288.6*	D'AF + 90
43	An	14.91	39.02	2	110	3/3	121.8	−60.4	1528	3.0	12.2	280.0*	D'AF + 90
45	An	14.91	39.02	10	095	4/4	091.9	−65.6	128	8.1	−09.7	278.0*	D'AF + 90
46	An	14.88	39.02	?	110	3/3	042.0	−75.6	162	9.7	−33.7	289.4*	D'AF + 90
47	An	14.88	39.02	20	050	3/3	057.0	−50.2	415	6.0	−35.6	258.7*	D'AF + 90
51	An	14.87	39.02	10	340	3/3	050.3	−67.2	913	4.0	−36.3	283.0*	D'AF + 90
Mean	An		*Olivença only*			28†	082.7	−71.4	42	4.3	−16.5	286.7*	$K = 16.4, A_{95} = 6.9°$
Mean	Ar		*Olivença only*			10†	301.9	61.9	42	7.5	11.4	282.6	$K = 20.2, A_{95} = 11.0°$
Mean	An + Ar		*Olivença only*			38†	276.0	69.9	31	4.3	−09.2	285.6	$K = 12.6, A_{95} = 6.8°$
All areas combined													
Mean	An		*All areas combined*			59†	071.9	−70.0	44	2.8	−22.3	284.6*	$K = 17.2, A_{95} = 4.6°$
Mean	An		*All areas combined, Ilhéus = 1 site*			33†	086.5	−72.3	38	4.1	−14.3	288.3*	$K = 14.3, A_{95} = 6.8°$
Mean	Ar		*All areas combined*			13†	299.9	62.1	51	5.9	10.2	282.0	$K = 24.7, A_{95} = 8.5°$
Mean	An + Ar		*All areas combined*			72†	262.5	69.8	32	3.0	−16.5	284.1	$K = 12.9, A_{95} = 4.8°$
Mean	An + Ar		*All areas combined, Ilhéus = 1 site*			46†	279.0	70.1	31	3.8	−07.3	286.4	$K = 12.5, A_{95} = 6.2°$

Notes: Comp., ChRM component abbreviation as defined in text (parentheses indicate exclusion from means); *w*, dyke width; strike/dip of dyke attitude in degrees; *n*/*N*, number of samples in mean direction/number analysed; GDec, GInc, mean ChRM in geographic coordinates (deg); *k*, a_{95}, Fisher's (1953) precision parameter and radius (deg) of the 95% cone of confidence about the mean direction; Plat, Plong, virtual geomagnetic pole latitude, longitude; D'AF + 90, 04, site passing quality filtering herein, from D'Agrella-Filho *et al.* (1990, 2004). U–Pb ages are from this study.
*Plat, Plong listed as antipole of the mean direction given in the table.
†Number of sites contributing to the mean direction. comb., combined result; undul., undulose geometry.

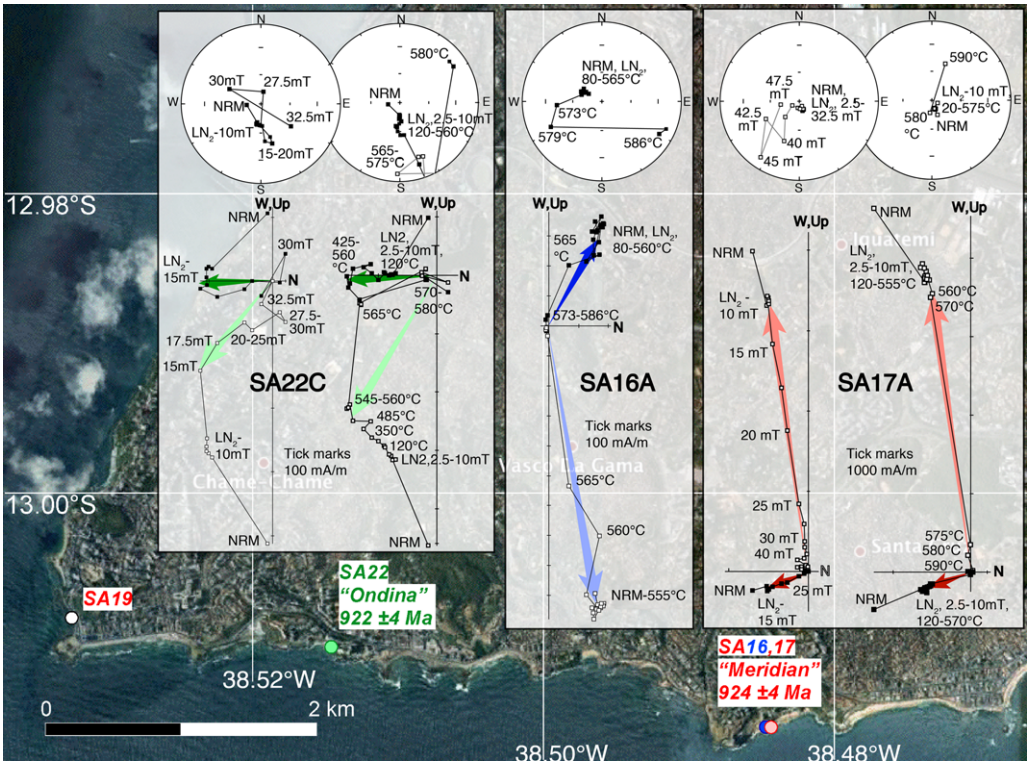

Fig. 5. Salvador palaeomagnetic data. Backdrop image from Google Earth™ shows sampling sites (with U–Pb ages reported herein), colour-coded by the characteristic remanence direction (red, A component 'normal'; blue, A component 'reversed'; green, C component). On equal-area stereoplots, solid symbols represent lower-hemisphere vectors and open symbols represent upper-hemisphere vectors. On orthogonal projection diagrams, solid symbols show projections onto the horizontal plane and open symbols show projections onto the vertical plane.

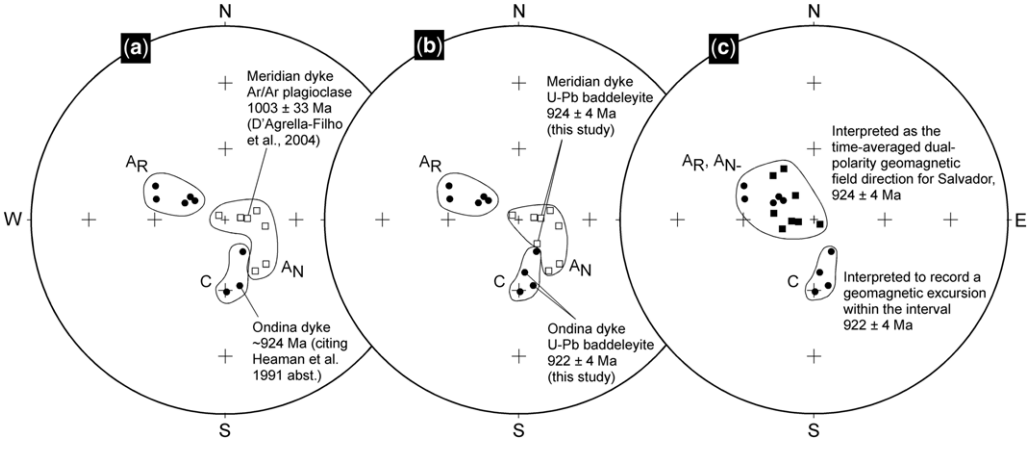

Fig. 6. Site-mean ChRM directions from Salvador (prior to quality filtering), grouped (**a**) according to D'Agrella-Filho *et al.* (2004), (**b**) according to this study, with new U–Pb ages indicated at sites with our independent confirmation of the previous palaeomagnetic directions, and (**c**) according to the geomagnetic interpretation of this study (square symbols show A_N site-mean directions reflected through the origin). Closed v. open symbols indicate lower- v. upper-hemisphere projections, respectively.

inferred 2° of vertical-axis rotation for the Salvador region accompanying Atlantic-Ocean rifting, we do not employ such a correction herein because it does not significantly affect our combined mean directions that rely much more heavily on the more abundantly sampled southern outcrop areas.

Ilhéus

D'Agrella-Filho *et al.* (1990) found very stable, very tightly clustered data from two areas around the city of Ilhéus. We resampled the more southerly of those two areas, around a coastal promontory known as Pernambuco Hill (Fig. 7), as well as an additional pair of dykes in a quarry SW of the city. Dykes are 0.5–12 m wide, and strike E to ENE. Our data from Ilhéus show very high stability to both AF and thermal demagnetization, and tight clustering of ChRM directions to the NE and steeply upward, which reproduces the earlier work of D'Agrella-Filho *et al.* (1990) (Table 2). Our site IL1 is from a 12 m-thick east-striking dyke that yielded the U–Pb baddeleyite age of 926.1 ± 4.6 Ma, reported above.

We undertook a baked-contact test on the dated dyke, into isolated pod-like amphibolite lenses within the Palaeoproterozoic gneiss host-rock adjacent to its southern margin (Fig. 7c). Samples of the host-rock were collected from within a few centimetres of the dyke margin, to distances as great as *c.* 40 m away. All host-rock samples yielded a ChRM direction that is slightly steeper than that of the dyke, but otherwise similar in its very stable demagnetization characteristics. We attribute the slight difference in directions to anisotropy in the amphibolite pods. The expected Palaeoproterozoic (*c.* 2.0 Ga) host-rock direction is steeply down to the NE (D'Agrella-Filho *et al.* 2004, 2011), and we did not find this direction in our baked-contact test at Pernambuco Hill. The results of this test, therefore, could be considered either negative or inconclusive. A primary age of remanence in the Ilhéus dykes would still be plausible if the overall density of dyke intrusion were great enough, or exposed crustal levels were deep enough, to remagnetize the entire outcrop area via magmatic heating. Lack of outcrop more than *c.* 40 m southward from the dated dyke also allows the possibility of additional dykes under cover, which could have contributed to the regional host-rock remagnetization.

Considering only the data from dykes (i.e. omitting baked-contacts), the mean of 27 sites (Fig. 7d) is $D = 058.4°$, $I = -66.0°$, $k = 161$, $a_{95} = 2.2°$. The corresponding mean of the 27 site-mean

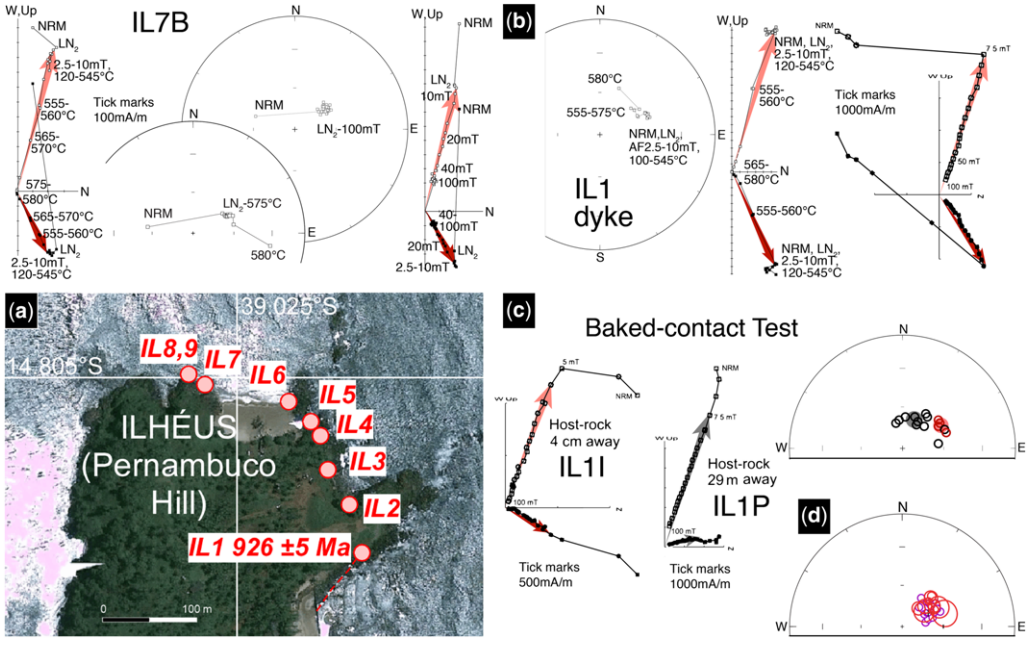

Fig. 7. Ilhéus palaeomagnetic data. (**a**) Site location map with Google Earth™ background. (**b**) Representative demagnetization data from dykes, plotted as both orthogonal projection diagrams and equal-area stereoplots. (**c**) Results of the baked-contact test into amphibolite pods within the Palaeoproterozoic basement gneiss. In the stereoplot, red symbols are from the dyke, whereas black symbols are from the amphibolites. (**d**) Equal-area stereoplot of site-means from this study (red) as compared with those of D'Agrella-Filho *et al.* 1990 (purple).

VGPs is at 31.8° S, 279.6°E, $K = 71$, $A_{95} = 3.3°$. This mean is notable in its high degree of precision: the angular dispersion parameter (s) is calculated as 9.6°, anomalously low relative to comparable palaeolatitudes from either the time-averaged field of the last 5 million years or typical Proterozoic data (Smirnov *et al.* 2011). We thus interpret the Ilhéus magnetizations as not averaging palaeosecular variation of the geomagnetic field at the time of remanence acquisition, so that this mean of VGPs in itself is regarded as merely a single VGP, not a time-averaged palaeomagnetic pole.

Olivença

Previous palaeomagnetic study of dykes exposed along the coast at Olivença (D'Agrella-Filho *et al.* 1990) documented a two-polarity ChRM directed either east-up (A-normal) or NW-down (A-reversed). The directions were found to be significantly not antiparallel. In addition, the A--reversed-magnetized dykes were mainly confined to a single section of coastline estimated to be 1–2 km in length, according to field notes from the original study. We resampled many of the Olivença dykes (Fig. 8) in order to fix the location of the polarity transitions as well as tie the palaeomagnetic data to new U–Pb ages. Dykes range from 0.3 to 24 m wide, and strike ENE (the two remanence polarity groups have indistinguishable strike means). Palaeomagnetic data are listed in Table 2. As with Salvador and Ilhéus, we generally reproduce the ChRM data from the older study of D'Agrella-Filho *et al.* (1990). Combining high-quality data from that study as well as new sites analysed herein, we compute the mean from 28 sites of A-normal ChRM directions at $D = 082.7°$, $I = -71.4°$, $k = 42$, $a_{95} = 4.3°$. The corresponding pole derived from the mean of the 28 VGPs is at 16.5° S, 286.7° E, $K = 16$, $A_{95} = 6.9°$. For 10 A-reversed sites in the combined Olivença dataset, the ChRM mean is $D = 301.9°$, $I = 61.9°$, $k = 42$, $a_{95} = 7.5°$, and the palaeomagnetic pole derived from VGPs is at 11.4° N, 282.6° E, $K = 20$, $A_{95} = 11.0°$. These combined data are not antiparallel, as also determined by D'Agrella-Filho *et al.* (1990), which will be discussed further below.

A baked-contact test was performed at site OL3, a 28 cm-wide mafic dyke intruding amphibolite host rocks towards the southern end of the Olivença sampling profile. As with the test at Ilhéus, similar steeply upward ChRM directions are obtained from host rocks as far as 6.5 m away from the dyke (Fig. 8c), much further than typical for a simple conductive heating profile at shallow to moderate levels of emplacement. Lack of outcrop beyond 6.5 m away allows the presence of additional dykes that could have contributed to regional remagnetization. A distant, isolated outcrop of amphibolite, *c.* 90 m away from the dyke (OL3x; Fig. 8b, bottom row), yielded a SW-shallow-up ChRM, very different from all other directions obtained in this study. We could perhaps consider this to indicate a positive result for the baked-contact test, but the following issues suggest caution. First, as noted above, the expected *c.* 2.0 Ga host rock directions are steeply down to the NE, substantially different from those observed in the isolated amphibolite outcrop. Second, in the earlier palaeomagnetic study of the region (D'Agrella-Filho *et al.* 1990), only one site gave a southwesterly and shallow direction (#70 in the Itaju do Colônia suite), and that site was located furthest south in the study area, closest to the northernmost Araçuaí orogenic front (Alkmim *et al.* 2006). It is possible that the isolated outcrop of amphibolite host rock retains a local hydrothermal record of Brasiliano (late Neoproterozoic) overprinting. Given these caveats, we must consider the Olivença baked-contact test as inconclusive.

Combined palaeomagnetic results

As noted above, site-mean palaeomagnetic data from Salvador and Ilhéus are each by themselves insufficient for statistical representation of the time-averaged Neoproterozoic geodynamo. Nonetheless, they may be combined with the more extensive Olivença dataset to produce a palaeomagnetic pole. Given that Ilhéus data, with their unusually high clustering of remanence directions and limited outcrop area, probably represent a single 'snapshot' of the *c.* 920 Ma geomagnetic field, we aggregate all of those data into a single mean direction with unit weight, equal to each of the quality-filtered sites from the two other regions (Table 2). The resulting means for the A-normal polarity direction ($n = 33$ sites, $D = 086.5°$, $I = -72.3°$, $k = 38$, $a_{95} = 4.1°$) and A-reversed polarity direction ($n = 13$ sites, $D = 299.9°$, $I = 62.1°$, $k = 51$, $a_{95} = 5.9°$) 'fails' the reversal test of McFadden & McElhinny (1990), in that directions are distinguishable from antiparallelism at >95% confidence (in fact, >99.9%). For this reason, and because we have only been able to separate and date baddeleyite from A-normal polarity dykes, we calculate separate palaeomagnetic poles for each of the 'A' remanence polarities in coastal Bahia (Table 3). The A-normal pole derived from the mean of the 33 site-mean VGPs is at 14.3° S, 288.3° E, $K = 14.3$, $A_{95} = 6.8°$.

Although baked-contact tests on A-normal remanence directions from the present study all proved to be inconclusive, D'Agrella-Filho *et al.* (2004) discuss the results of three baked-contact tests from Salvador. Two are presented as fully positive tests, with stable directions in both unbaked and

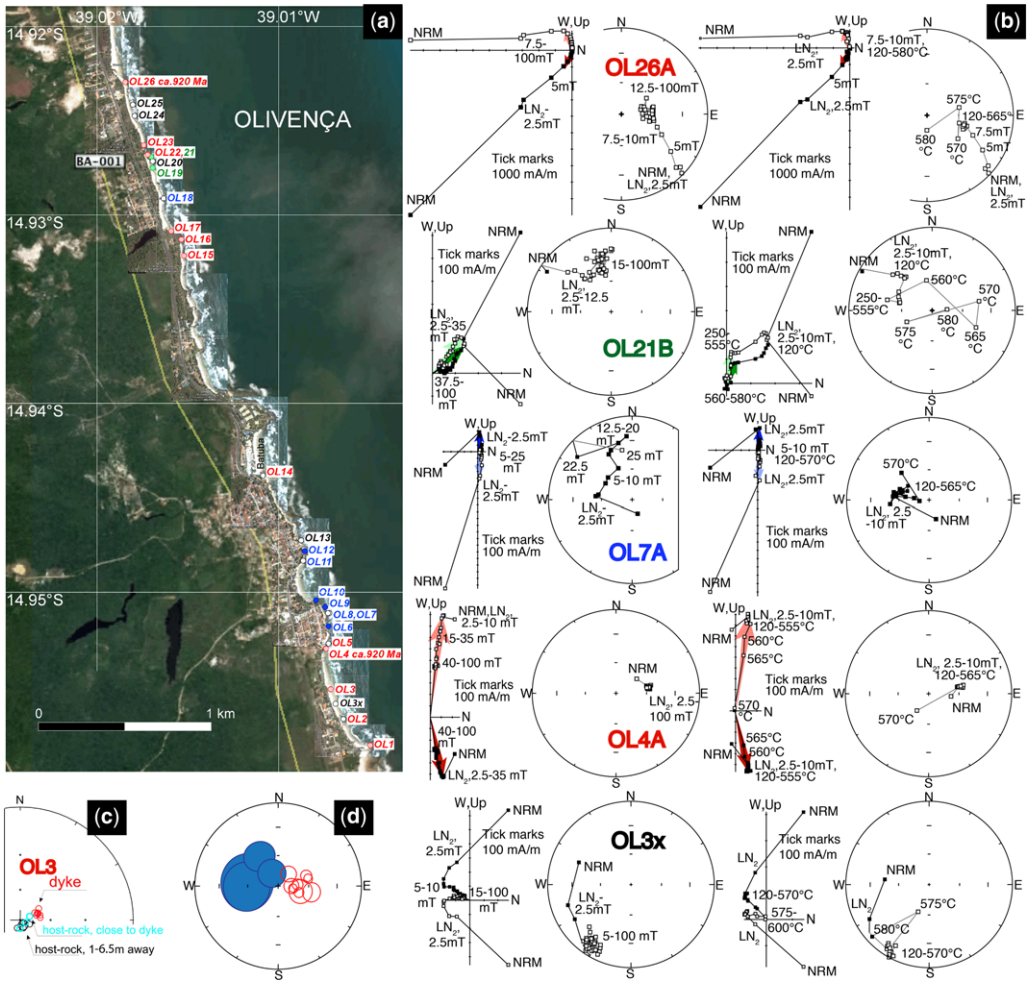

Fig. 8. Olivença palaeomagnetic data. (**a**) Site location map with Google Earth^{TM} background. (**b**) Representative demagnetization data from dykes, plotted as both orthogonal projection diagrams and equal-area stereoplots. (**c**) Results of the baked-contact test into amphibolite pods within the Palaeoproterozoic basement gneiss. In the stereoplot, red symbols are from the 28 cm-wide dyke and light blue and black symbols are from the amphibolites. (**d**) Equal-area stereoplot of site-means from this study, in the lower hemisphere (solid blue ovals, 'reversed' polarity) and upper hemisphere (open red, 'normal').

baked host Palaeoproterozoic gneisses, the latter group aligned with remanence directions from A-reversed dykes at sites 8 and 16. These data demonstrate that the A-reversed direction is primary, dating from the time of dyke cooling immediately following intrusion. A third attempted baked-contact test by D'Agrella-Filho *et al.* (2004), on granulitic host rocks to the thick 'Meridian' dyke with A-normal polarity, was judged to be inconclusive owing to distant host rocks not yielding a stable direction. However, sites 16 and 17 are from the same beach cove; thus the magnetically stable, unbaked granulite samples pertinent to the test at site 16 – although originally not considered as part of the test profile for site 17 – are in fact integral to a positive baked contact test for that thicker dyke.

Both A-normal and A-reversed remanence polarities, therefore, are arguably primary. Both poles are similar to Early Cambrian poles from the Congo craton (Meert & Van der Voo 1996), when viewed in a common Gondwana-Land reference frame (McElhinny *et al.* 2003), but the coastal Bahia study area entirely lacks any evidence for significant Cambrian (latest Brasiliano) structural or thermal disturbance (Renne *et al.* 1990). Our U–Pb ages now date the emplacement of A-normal dykes as

Table 3. *Selected c. 950–900 Ma palaeomagnetic poles from SF/Congo and Baltica*

Rock unit	Code	Age (Ma)	Method	Latitude (°N)	Longitude (°E)	A_{95} (deg)	1234567 Q	Palaeomagnetic reference	Geochronology reference
São Francisco/ Congo									
Bahia coastal A-normal	BA-n	*c.* 920	U–Pb	−14	288	7	1111100 5	This study	This study
Bahia coastal A-reversed	BA-r	1080–920	Ar/Ar, U–Pb	10	282	6	0111100 4	This study	This study; Renne *et al.* (1990)
Bahia coastal A (2-polar)	BA	920?	U–Pb	−07	286	6	1111110 6	This study	This study
Itaju do Colônia	IC	*c.* 920?	Correl.	−08	291	10	0110110 4	D'Agrella-Filho *et al.* (1990)	This study
Nyabikere pluton*	Nya	*c.* 950?	Ar/Ar	−17	258	11	1010000 2	Meert *et al.* (1994)	Meert *et al.* (1994)
Baltica									
Rogaland complex	Rog	*c.* 870	Cooling	46	058	18	1111001 5	Walderhaug *et al.* (2007)	Walderhaug *et al.* (2007)
Egersund–Ogna	EgO	*c.* 900	Cooling	42	020	9	1110001 4	Brown & McEnroe (2004)	Brown & McEnroe (2004)
Hakefjorden intrusions	Hak	916 ± 11	U–Pb	−05	069	4	1110001 4	Stearn & Piper (1984)	Scherstén *et al.* (2000)
Southern Swedish dykes	SSD	946–935	U–Pb	01	061	7	1111111 7	Elming *et al.* (2014)	Elming *et al.* (2014)

Notes: correl., correlation of undated rocks to others in the table with direct age constraints. Given the slight difference in pole position of the 'reversed' Bahia-coastal dykes, it remains possible that it could have a substantially different age from the *c.* 920 U–Pb dates on 'normal' polarity dykes in the same region. The $^{40}Ar/^{39}Ar$ age on 'reversed' dykes (Renne *et al.* 1990) is thus assumed as an approximate maximum constraint for that polarity.

*Rotated to São Francisco reference frame using Euler parameters (46.8°, 329.4°, −55.9°) from McElhinny *et al.* (2003).

c. 920 Ma, thus the Bahia coastal A-normal pole (Table 3) is considered to be the most reliable palaeomagnetic result from the early Neoproterozoic SF/Congo craton. We calculate the dual-polarity combined mean of Bahia coastal A-normal and A-reversed dykes, but we caution against use of that pole without U–Pb dating of the A-reversed dykes. Inland from the coast, the Itaju do Colônia dykes have dual polarity with demonstrable antiparallelism, but these, too, remain undated.

Discussion

Neoproterozoic large igneous province

This study reports new U–Pb baddeleyite ages for five diabase dykes from the coastal Bahia swarm(s) that vary between 926 and 918 Ma, the ages overlapping within analytical uncertainty. The short duration for emplacement of this magmatism (<8 myr) appears to justify grouping all of the coastal Bahia dykes into a single intraplate magmatic event, proposed as a possible large igneous province (LIP) in Ernst & Buchan (1997), for which we propose an emplacement age of 923.2 ± 2.6 Ma (weighted mean of our new dates; MSWD = 1.6). The ages are significantly younger than previous $^{40}Ar/^{39}Ar$ biotite and plagioclase stepwise heating results from the same swarms (Renne *et al.* 1990; D'Agrella-Filho *et al.* 2004). Previous studies have shown that many of these dykes have disturbed K–Ar and $^{40}Ar/^{39}Ar$ dates; in some cases younger dates are recorded that reflect a Neoproterozoic Brasiliano disturbance, for example some diabase plagioclase analyses that record dates of *c.* 650 Ma (Renne *et al.* 1990), and in other cases older dates are recorded, probably a consequence of the presence of excess argon that appears pervasive in the region (summarized in D'Agrella-Filho *et al.* 2004).

Salvador, Ilhéus and Olivença dykes have been considered to represent a radiating (Bahia) swarm converging on the eastern margin of the São Francisco craton (e.g. Ernst & Buchan 1997). Our new geochronology supports this model, in which the various Bahia dyke swarms may converge towards an interpreted 920 Ma mantle plume centre located near the northern apex of the Araçuaí–West Congo orogen (Fig. 1). On the other side of the cratonic 'bridge' in a pre-Atlantic restoration, the Congo craton hosts the 920 Ma Gangila basalts and overlying Mayumbian rhyolites in the West Congo belt, which have geochemistry similar to continental flood magmas (Tack *et al.* 2001). Taken together, the *c.* 920 Ma radiating swarm of the São Francisco craton, and coeval Mayumbian–Gangila magmatism of the Congo craton, delineate the minimum areal extent of the magmatism to be 350 000 km^2 (Ernst *et al.* 2008), which is much larger than the minimum size of 100 000 km^2 required to be called a LIP (Coffin & Eldholm 1994; Bryan & Ernst 2008). Machado *et al.* (1989) obtained a U–Pb zircon–baddeleyite combined age of 906 ± 2 Ma from a mafic body in the Espinhaço region, several hundred kilometres to the SW. Extensional granitoids within the northern Araçuaí orogen are somewhat younger, dated by SHRIMP U–Pb on zircons at 875 ± 9 Ma (da Silva *et al.* 2008). Initial phases of sedimentation in the Macaúbas Group, within the Araçuaí orogen, appear to have begun at about this time (Pedrosa-Soares & Alkmim 2011). Sedimentation within spoke-like aulacogens radiating from the Araçuaí–West Congo orogen also appears to be related to this regional extension (Alkmim & Martins-Neto 2012); for example, the northern Paramirim aulacogen contains mafic magmatism dated by SHRIMP U–Pb on zircon at 854 ± 23 Ma (MSWD = 6.7; Danderfer *et al.* 2009).

Undated dykes in the Congo craton could also possibly be members of the 920 Ma LIP. Specifically, possible correlatives are swarms at Ebolowa (Cameroon), Sembe-Ouesso and Comba (Democratic Republic of Congo). A tree-like branching pattern for these dykes (extending over an area of 1200 by 800 km), in the standard reconstruction of the Mesoproterozoic São Francisco and Congo cratons, is envisioned by Correa-Gomes & Oliveira (2000). However, precise dating is required before any conclusions can be drawn about swarm geometry in the Congo portion of the *c.* 920 Ma LIP. D'Agrella-Filho *et al.* (1996) found a distinct palaeomagnetic remanence direction from unmetamorphosed dykes in Gabon, which if primary would indicate a significantly different age from the Bahia dykes investigated herein, and reinforce the possibility that more than one LIP event may be recorded by post-Palaeoproterozoic dykes in the western SF/Congo craton.

SF/Congo apparent polar wander path

Our U–Pb ages correspond to Bahia dykes carrying the 'A-normal' and 'C' palaeomagnetic remanence directions, from all three sampled regions (Salvador, Ilhéus and Olivença). The discrepancy between A-normal and C directions corresponds to *c.* 50° of arc distance between virtual geomagnetic poles (Fig. 9), despite the indistinguishable U–Pb ages. The uncertainties on those ages could be stretched to their limits in an attempt to explain the palaeomagnetic discordance by rapid plate motions or true polar wander (see similar discussion in Swanson-Hysell *et al.* 2009), but we suggest that in this case the most parsimonious interpretation is that the 'C' direction represents a geomagnetic

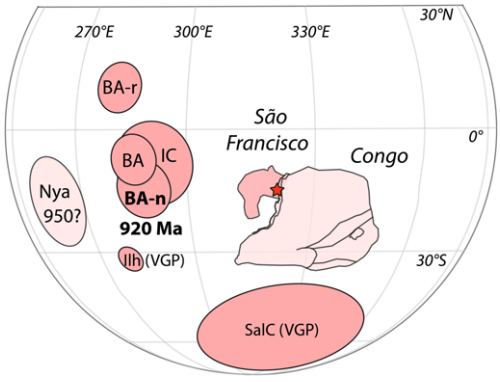

Fig. 9. Revised ages of early Neoproterozoic palaeomagnetic poles from the SF/Congo craton, in present South American coordinates (Tables 2 & 3). Star indicates the generalized location of sampling localities. Pole abbreviations match those in Table 3, plus the two virtual geomagnetic poles (VGPs) from Ilhéus (Ilh) and the Salvador 'C' component (SalC).

excursion sampled by three dykes (known thus far) in Salvador.

Similarly, time-averaging of the Proterozoic geomagnetic field can be questioned for the Ilhéus A-normal data. D'Agrella-Filho *et al.* (1990) discussed two alternative explanations for the exceptionally tight clustering of Ilhéus ChRM directions: either they record a mere 'snapshot' of the Proterozoic geomagnetic field owing to emplacement within a time span substantially less than a few thousand years, or ambient crustal temperatures at the time of emplacement were so high that the ChRMs were acquired over a protracted cooling period that tended to average palaeosecular variation of the field within each specimen's range of iron oxide grain sizes. These models have opposing implications for tectonic reconstruction purposes; either the mean direction does not point to the Earth's rotation axis at *c.* 920 Ma, or it does. Given the conclusions from Salvador that suggest a large geomagnetic excursion recorded by the C direction, we suggest that the Ilhéus A-normal data represent another 'snapshot' of the field that also does not coincide with the Earth's rotation axis at that time. Whether these results imply that the *c.* 920 Ma geomagnetic field was particularly prone to excursions, will be discussed further in relation to coeval data from other cratons, below. We note that both the Salvador C and Ilhéus A-normal virtual geomagnetic poles are displaced in approximately the same azimuth from the mean dual-polarity 'A' pole from Salvador, and may indicate a palaeomeridian of preferred directions of the reversal-transitional field akin to that of the past few million years (Love 2000; Hoffman & Singer 2008).

Although several A-reversed dykes were sampled for geochronology, no baddeleyite has yet been recovered from those units. The asymmetry of A-normal and A-reversed directions from Olivença was ascribed to an age difference of 60–70 myr between those dykes (D'Agrella-Filho *et al.* 1990), consistent with the available $^{40}Ar/^{39}Ar$ data in the companion study (Renne *et al.* 1990). According to that model, the A-reversed dykes would have intruded as a narrow swarm centred on Olivença, and then tens of millions of years later, the A-normal dykes would have intruded neatly on both sides of the older swarm but systematically avoided the zone of earlier emplacement. This could be plausible if 'rift hardening' had occurred, by which the density of dyke intrusions in the central zone affected the material properties of the crust so as to preclude invasion by the younger dykes (see discussion of a variety of possible mechanisms, in Yamasaki & Stephenson 2009). Alternatively, we suggest that the Olivença ChRM polarity profile could be equally well explained by a north-to-south or south-to-north propagation of magmatism encompassing two geomagnetic field reversals. In this model, the A-reversed and A-normal directions should be nearly equivalent in age, and dated to *c.* 920 Ma by our U–Pb results from the southern A-normal zone. The asymmetry in Olivença 'A' directions, then, would need to be explained by geomagnetic secular variation, for which compelling evidence exists in the Salvador and Ilhéus datasets as noted above.

Summary palaeomagnetic poles from Bahia are listed in Table 3. Our new results profoundly alter the Meso-Neoproterozoic database for the SF/Congo craton. If the U–Pb ages reported herein are to be used rather than the older $^{40}Ar/^{39}Ar$ data, then the A-normal directions correspond to *c.* 920 Ma, and there is no longer any *c.* 1010 Ma pole from SF/Congo. The A-reversed direction is either penecontemporaneous with A-normal (as suggested by the Itaju do Colônia dataset), or older, in which case the *c.* 1080 Ma $^{40}Ar/^{39}Ar$ age on Olivença A-reversed dykes (Renne *et al.* 1990) might still be relevant to that direction. The Salvador 'C' direction, preserved in three dykes, was posited by D'Agrella-Filho *et al.* (2004) to represent the latitude and orientation of the SF/Congo craton at *c.* 920 Ma, but herein we provide evidence that it merely represents a geomagnetic excursion, since it differs so greatly from the much more abundant A-normal direction of indistinguishable age. Only one other early Neoproterozoic pole exists from the SF/Congo craton; the Nyabikere pluton VGP (Meert *et al.* 1994) derives from one site with no tilt control. No other localities bear the same 'anomalous' direction, which is interpreted to represent a thermal overprint dated by $^{40}Ar/^{39}Ar$

geochronology at *c.* 950 Ma. In the São Francisco reference frame, the Nyabikere VGP (Table 3) is similar to the 920 Ma poles refined herein (Fig. 9).

Implications for Rodinia

The new ages and palaeomagnetic data reported herein carry important implications for Rodinia supercontinent reconstructions. Our discussion of possible pole/age comparisons relies on the global compilations of palaeomagnetic data by Li *et al.* (2008) and Evans (2009). In general, very few data exist for the *c.* 920 Ma interval of relevance to our new results. The age of 920 Ma, in itself, may find a match in precisely coeval mafic dykes of the North China craton (Peng *et al.* 2011), although no palaeomagnetic data from the North China dykes are available to test that correlation. The Cuizhuang/Sanjiaotang sedimentary formations, also from North China, have a palaeomagnetic pole that was earlier estimated to be *c.* 950 Ma (Zhang *et al.* 2006), but recent U–Pb geochronology demonstrates those formations to be Palaeoproterozoic in age (Su *et al.* 2012).

In Laurentia, granitic magmatism of *c.* 950–930 Ma age is widespread in East Greenland (Watt & Thrane 2001) and East Svalbard (Johansson *et al.* 2005), although the magmatism is accompanied by deformation and mafic dykes of that age have not yet been found; thus the tectonic character of magmatism is quite distinct from that of SF/Congo at the same age. No palaeomagnetic data are available from those granitic rocks. The so-called Grenville Loop of Laurentian APW was long regarded as *c.* 900 Ma in age, but more recent thermochronology indicates that the apex of the loop is *c.* 1000 Ma (Warnock *et al.* 2000; Brown & McEnroe 2012), too old for comparison with the present study. The Oaxaquia anorthosite palaeomagnetic pole (Ballard *et al.* 1989) has also been assigned an age of about 950 Ma, but the pole is not precisely dated, and the tectonic association of Oaxaquia in Rodinia is not straightforward.

The best palaeomagnetic comparisons that can be made to the Bahia coastal dykes are to be found within Baltica. Mafic dykes of similar age are found in southern Sweden, in the foreland to the Sveconorwegian orogen, and palaeomagnetic data are available from those units (Pisarevsky & Bylund 2006; Elming *et al.* 2014). Early Neoproterozoic sedimentary rocks of the southern Urals also have yielded palaeomagnetic data (Pavlov & Gallet 2010), but the ages of those units are not well constrained.

Interestingly, the Sveconorwegian mafic palaeomagnetic record also indicates a swath of directions distributed over tens of degrees of arc length. The closest age matches in southern Sweden and Norway, as compared with 920 Ma for SF/Congo determined herein, are from the Blekinge–Dalarna dykes at 946–939 Ma (Elming *et al.* 2014), the Göteborg–Slussen dykes at 935 ± 3 Ma (Pisarevsky & Bylund 2006) and the Hakefjorden intrusions at 916 ± 11 (Stearn & Piper 1984; age from Scherstén *et al.* 2000). We follow Brown & McEnroe (2004), Pisarevsky & Bylund (2006), and Walderhaug *et al.* (2007) in assigning the Rogaland complex mean poles to an age significantly younger than that suite's U–Pb zircon determinations of *c.* 930 Ma (Schärer *et al.* 1996), perhaps as young as *c.* 900–870 Ma, owing to slow regional cooling of that internal zone in the Sveconorwegian orogen (Walderhaug *et al.* 2007).

The Southern Swedish dykes (SSD; Table 3; Fig. 10) key palaeomagnetic pole, at *c.* 940 Ma, is bolstered by positive baked-contact tests (Elming *et al.* 2014). One older dyke at Karlshamn, dated by U–Pb at 954 ± 1 Ma, yields a distinct virtual geomagnetic pole that is considered by Pisarevsky & Bylund (2006) to record a geomagnetic excursion (Fig. 10). Aside from that anomaly, the Baltica poles show a consistent pattern of migration, from low–moderate palaeolatitudes at 966–916 Ma to high palaeolatitudes by *c.* 900–870 Ma (Brown & McEnroe 2004; Pisarevsky & Bylund 2006; Walderhaug *et al.* 2007; Elming *et al.* 2014).

The most appropriate palaeomagnetic pole match between SF/Congo and Baltica is our new Bahia A-normal pole (BAn) at 920 Ma, and interpolation of the SSD and Hakefjorden poles dated at *c.* 940 and 916 ± 11 Ma, respectively (Table 3). These comparisons permit a direct test of the Rodinia reconstructions by Li *et al.* (2008) and Evans (2009). Figure 10 shows such tests, which fail (i.e. the Bahia dykes A-normal pole does not overlap the Baltica poles) in both cases; minor adjustments to the locations in each reconstruction could accommodate the new data, but other cratons' positions would also need to be adjusted to make room for the modified location of SF/Congo.

Figure 11 shows a range of possible reconstructions of SF/Congo according to the 920 Ma palaeolatitude from the Bahia dykes A-normal pole, and exercising freedom of both palaeolongitude and absolute geomagnetic polarity. The figure also shows Baltica in its SSD-defined palaeolatitude and orientation, as well as Laurentia attached to Baltica in a 'right-way-up' juxtaposition (Cawood & Pisarevsky 2006). Despite many controversies surrounding Neoproterozoic supercontinent reconstructions, this 'right-way-up' model of Laurentia and Baltica appears to be the most agreed upon (Piper 2007; Li *et al.* 2008; Evans 2009), and indeed, it has the greatest scholarly longevity among the currently viable Neoproterozoic cratonic juxtapositions (first proposed by Ueno *et al.* 1975).

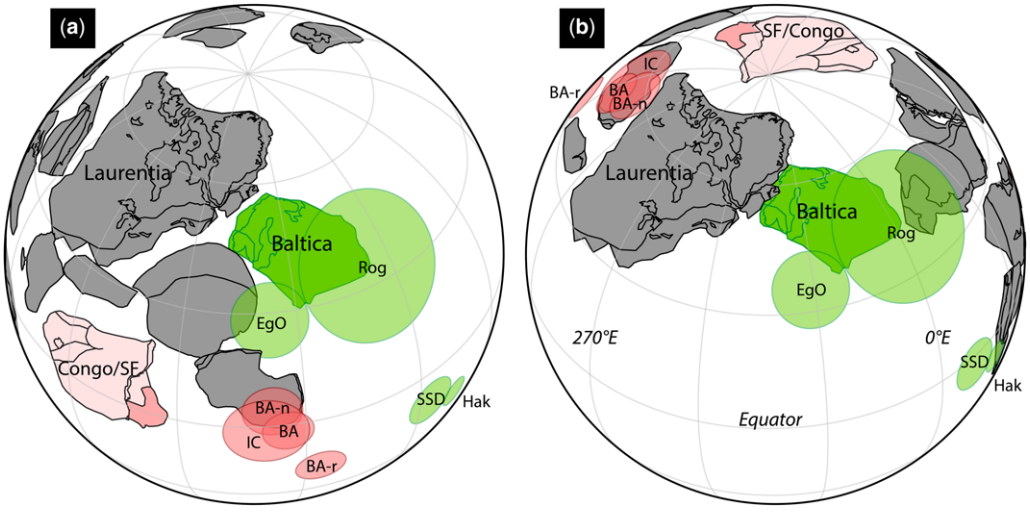

Fig. 10. Palaeomagnetic tests of proposed Rodinia reconstructions at *c.* 920 Ma, from (**a**) Li *et al.* 2008; and (**b**) Evans 2009. Both panels show Laurentia in present coordinates, with 30° grid lines. Pole abbreviations as in Table 3 and Figure 9.

From Figure 11 it is seen that several possible positions of SF/Congo could merit its inclusion within a Rodinia landmass at 920 Ma. Each of those alternatives would make different predictions regarding the duration of the reconstruction. For example, positions (b) and (g) juxtapose the NE margin of Congo with either cratonic Laurentia or Baltica, respectively. Since none of those margins contains a late Mesoproterozoic suture, the hypothesized juxtaposition should extend to pre-Rodinia times, perhaps as old as Palaeoproterozoic. Positions (c) and (f), however, juxtapose the Irumide margin of Congo with either Laurentia or Baltica. In those models, the Irumide orogeny would be a likely candidate for establishment of the juxtaposition at *c.* 1020 Ma (De Waele *et al.* 2009); hence one would not expect geological or palaeomagnetic matches for pre-Rodinia times. Comprehensive exploration of all of these possibilities is beyond the scope of this paper.

The classical basis for a palaeomagnetic comparison between Laurentia and right-way-up

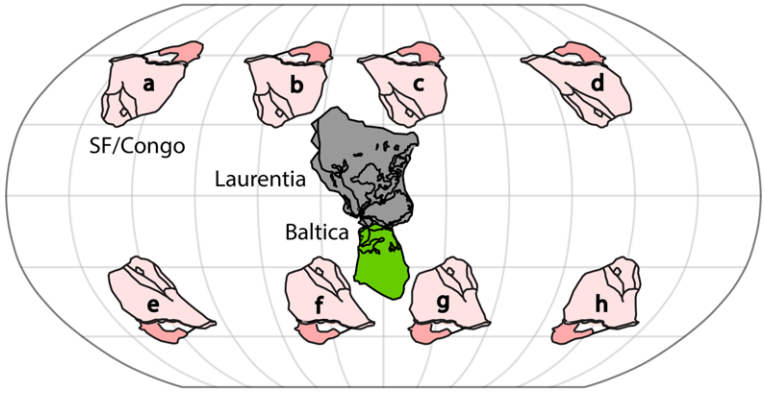

Fig. 11. Plausible (partial) Rodinia reconstructions including the SF/Congo craton, using the dual-polarity Bahia dykes pole from this study. Baltica and Laurentia are in the 'right-way-up' relative configuration (Cawood & Pisarevsky 2006) using the Euler parameters of Evans (2009), restored to the absolute frame according to the southern Swedish dykes mean pole (Elming *et al.* 2014). Grid lines are 30°, and absolute palaeolongitude is arbitrary. Possible positions of SF/Congo, labelled (a)–(h), are discussed in text.

Baltica is the superposition of the Grenville APW loop with its Sveconorwegian counterpart from Baltica (Ueno *et al.* 1975). As with the Sveconorwegian, much debate surrounds the timing and sense of rotation around the Grenville loop (e.g. Hyodo & Dunlop 1993; Weil *et al.* 1998), but the most recent data suggest its timing to be entirely older than the Sveconorwegian loop (Brown & McEnroe 2012; Elming *et al.* 2014). If we are to accept a right-way-up reconstruction of Baltica against Laurentia during the assembly and tenure of Rodinia, then, we must accept a joint APW path with numerous parallel oscillations between 1000 and 900 Ma.

Many of the Grenville and Sveconorwegian palaeomagnetic data derive from high-grade crystalline rocks or plutons that may have cooled slowly through that interval of time. The palaeomagnetic record from more quickly cooled dykes in cratonic Baltica (Elming *et al.* 2014) and SF/Congo craton (this study) from the same time intervals may contribute substantially to the ambiguities presented by those APW loops. Our study may, therefore, provide a broader perspective towards the question of large palaeomagnetic variance in several intervals of Neoproterozoic time (most notably the Ediacaran Period), for which a variety of alternative explanations have been postulated: rapid plate tectonics (Meert *et al.* 1993), oscillatory true polar wander (Evans 1998, 2003) or non-uniformitarian geodynamo (Abrajevitch & Van der Voo 2010). Detailed palaeomagnetic study of precisely dated mafic dykes may hold the key to answering these issues.

We thank L. Evans for assistance in the field, and J. Dalton de Souza (CPRM) for logistical support. P. Hollings provided valuable comments on a draft version of the manuscript. D.E. was funded by the David & Lucile Packard Foundation. The U–Pb geochronology research at the University of Alberta was funded by an NSERC Discovery Grant to L.M.H.. Other U–Pb ages were supported by the Industry–Academia–Government–Consortium project 'Reconstruction of Supercontinents Back to 2.7 Ga Using the Large Igneous Province (LIP) Record: with Implications for Mineral Deposit Targeting, Hydrocarbon Resource Exploration and Earth System Evolution' (www.supercontinent.org). This is publication no. 39 of that project.

References

Abrajevitch, A. & Van der Voo, R. 2010. Incompatible Ediacaran paleomagnetic directions suggest an equatorial geomagnetic dipole hypothesis. *Earth and Planetary Science Letters*, **293**, 164–170.

Alkmim, F. F. & Martins-Neto, M. A. 2012. Proterozoic first-order sedimentary sequences of the São Francisco craton, eastern Brazil. *Marine and Petroleum Geology*, **33**, 127–139.

Alkmim, F. F., Marshak, S., Pedrosa-Soares, A. C., Peres, G. G., Cruz, S. & Whittington, A. 2006. Kinematic evolution of the Araçuaí–West Congo orogen in Brazil and Africa: nutcracker tectonics during the Neoproterozoic assembly of Gondwana. *Precambrian Research*, **149**, 43–64.

Ballard, M. A., Van der Voo, R. & Urrutia-Fucugauchi, J. 1989. Paleomagnetic results from Grenvillian-aged rocks from Oaxaca, Mexico: evidence for a displaced terrane. *Precambrian Research*, **42**, 343–352.

Brown, L. L. & McEnroe, S. A. 2004. Palaeomagnetism of the Egersund–Ogna anorthosite, Rogaland, Norway, and the position of Fennoscandia in the late Proterozoic. *Geophysical Journal International*, **158**, 479–488.

Brown, L. L. & McEnroe, S. A. 2012. Paleomagnetism and magnetic mineralogy of Grenville metamorphic and igneous rocks, Adirondack Highlands, USA. *Precambrian Research*, **212–213**, 57–74.

Bryan, S. & Ernst, R. E. 2008. Revised definition of Large Igneous Provinces (LIPs). *Earth-Science Reviews*, **86**, 175–202.

Cawood, P. A. & Pisarevsky, S. A. 2006. Was Baltica right-way-up or upside-down in the Neoproterozoic? *Journal of the Geological Society, London*, **163**, 1–7.

Coffin, M. F. & Eldholm, O. 1994. Large igneous provinces: crustal structure, dimensions, and external consequences. *Reviews of Geophysics*, **32**, 1–36.

Cordani, U. G., D'Agrella-Filho, M. S., Brito-Neves, B. B. & Trindade, R. I. F. 2003. Tearing up Rodinia: the Neoproterozoic palaeogeography of South American cratonic fragments. *Terra Nova*, **15**, 350–359.

Correa-Gomes, L. C. & Oliveira, E. P. 2000. Radiating 1.0 Ga mafic dyke swarms of eastern Brazil and western Africa: evidence of post-assembly extension in the Rodinia supercontinent? *Gondwana Research*, **3**, 325–332.

D'Agrella-Filho, M. S. 1992. *Paleomagnetismo de enxames de diques máficos Proterozóicos e rochas do embasamento do cráton do São Francisco*. PhD thesis, Departamento de Geofísica, IAG-USP, São Paulo, SP, Brasil, 201pp.

D'Agrella-Filho, M. S., Pacca, I. G., Renne, P. R., Onstott, T. C. & Teixeira, W. 1990. Paleomagnetism of Middle Proterozoic (1.01 to 1.08 Ga) mafic dykes in southeastern Bahia State – São Francisco Craton, Brazil. *Earth and Planetary Science Letters*, **101**, 332–348.

D'Agrella-Filho, M. S., Feybesse, J. L., Prian, J. P., Dupuis, D. & N'Dong, J. E. 1996. Paleomagnetism of Precambrian rocks from Gabon, Congo craton, Africa. *Journal of African Earth Sciences*, **22**, 65–80.

D'Agrella-Filho, M. S., Trindade, R. I. F., Siqueira, R., Ponte-Neto, C. F. & Pacca, I. G. 1998. Paleomagnetic constraints on the Rodinia supercontinent: implications for its Neoproterozoic break-up and the formation of Gondwana. *International Geology Review*, **40**, 171–188.

D'Agrella-Filho, M. S., Pacca, I. I. G., Trindade, R. I. F., Teixeira, W., Raposo, M. I. B. & Onstott, T. C. 2004. Paleomagnetism and $^{40}Ar/^{39}Ar$ ages of mafic dikes from Salvador (Brazil): new constraints

on the São Francisco craton APW path between 1080 and 1010 Ma. *Precambrian Research*, **132**, 55–77.

D'Agrella-Filho, M. S., Trindade, R. I. F., Tohver, E., Janikian, L., Teixeira, W. & Hall, C. 2011. Paleomagnetism and $^{40}Ar/^{39}Ar$ geochronology of the high-grade metamorphic rocks of the Jequié block, São Francisco Craton: Atlantica, Ur and beyond. *Precambrian Research*, **185**, 183–201.

Dalziel, I. W. D. 1997. Neoproterozoic–Paleozoic geography and tectonics: review, hypothesis, environmental speculation. *Geological Society of America Bulletin*, **109**, 16–42.

Danderfer, A., De Waele, B., Pedreira, A. J. & Nalini, H. A. 2009. New geochronological constraints on the geological evolution of Espinhaço basin within the São Francisco Craton – Brazil. *Precambrian Research*, **170**, 116–128.

da Silva, L. C., Pedrosa-Soares, A. C., Teixeira, L. R. & Armstrong, R. 2008. Tonian rift-related, A-type continental plutonism in the Araçuaí Orogen, eastern Brazil: new evidence for the breakup stage of the São Francisco–Congo Paleocontinent. *Gondwana Research*, **13**, 527–537.

Day, R., Fuller, M. & Schmidt, V. A. 1977. Hysteresis properties of titanomagnetites: grain size and compositional dependence. *Physics of the Earth and Planetary Interiors*, **13**, 260–267.

De Waele, B., Johnson, S. P. & Pisarevsky, S. A. 2008. Palaeoproterozoic to Neoproterozoic growth and evolution of the eastern Congo Craton: its role in the Rodinia puzzle. *Precambrian Research*, **160**, 127–141.

De Waele, B., Fitzsimons, I. C. W., Wingate, M. T. D., Tembo, F., Mapani, B. & Belousova, E. A. 2009. The geochronological framework of the Irumide Belt: a prolonged crustal history along the margin of the Bangweulu Craton. *American Journal of Science*, **309**, 132–187.

Elming, S.-Å., Pisarevsky, S. A., Layer, P. & Bylund, G. 2014. A palaeomagnetic and $^{40}Ar/^{39}Ar$ study of mafic dykes in southern Sweden: a new Early Neoproterozoic key-pole for the Baltic Shield and implications for Sveconorwegian and Grenville loops. *Precambrian Research*, **244**, 192–206.

Ernst, R. E. & Buchan, K. L. 1997. Giant Radiating Dyke Swarms: their use in identifying pre-Mesozoic large igneous provinces and mantle plumes. *In*: Mahoney, J. & Coffin, M. (eds) *Large Igneous Provinces: Continental, Oceanic, and Planetary Volcanism*. American Geophysical Union, Washington, DC, Geophysical Monographs, **100**, 297–333.

Ernst, R. E., Wingate, M. T. D., Buchan, K. L. & Li, Z. X. 2008. Global record of 1600–700 Ma Large Igneous Provinces (LIPs): implications for the reconstruction of the proposed Nuna (Columbia) and Rodinia supercontinents. *Precambrian Research*, **160**, 159–178.

Evans, D. A. 1998. True polar wander, a supercontinental legacy. *Earth and Planetary Science Letters*, **157**, 1–8.

Evans, D. A. D. 2003. True polar wander and supercontinents. *Tectonophysics*, **362**, 303–320.

Evans, D. A. D. 2009. The palaeomagnetically viable, long-lived and all-inclusive Rodinia supercontinent reconstruction. *In*: Murphy, J. B., Keppie, J. D. & Hynes, A. (eds) *Ancient Orogens and Modern Analogues*. Geological Society, London, Special Publications, **327**, 371–404.

Fernandez-Alonso, M., Cutten, H., De Waele, B., Tack, L., Tahon, A., Baudet, D. & Barritt, S. D. 2012. The Mesoproterozoic Karagwe–Ankole Belt (formerly the NE Kibara Belt): the result of prolonged extensional intracratonic basin development punctuated by two short-lived far-field compressional events. *Precambrian Research*, **216–219**, 63–86.

Fisher, R. A. 1953. Dispersion on a sphere. *Proceedings of the Royal Society of London, Series A*, **217**, 295–305.

French, J. E. & Heaman, L. M. 2010. Precise U–Pb dating of Paleoproterozoic mafic dyke swarms of the Dharwar Craton, India: implications for the existence of the supercraton Sclavia. *Precambrian Research*, **183**, 416–441.

Heaman, L. 1991. U–Pb dating of giant radiating dyke swarms: potential for global correlation of mafic magmatic events. *In*: *Extended Abstracts, International Symposium on Mafic Dykes, São Paulo, Brazil*, 7–9.

Heaman, L. M. & Machado, N. 1992. Timing and origin of Midcontinent Rift alkaline magmatism, North America: evidence from the Coldwell Complex. *Contributions to Mineralogy and Petrology*, **110**, 289–303.

Hoffman, K. A. & Singer, B. S. 2008. Magnetic source separation in Earth's outer core. *Science*, **321**, 1800.

Hoffman, P. F. 1991. Did the breakout of Laurentia turn Gondwanaland inside-out? *Science*, **252**, 1409–1412.

Hoffman, P. F. & Halverson, G. P. 2008. The Otavi Group of the Northern Platform and the Northern Margin Zone. *In*: Miller, R. McG. (ed.) *The Geology of Namibia*. Geological Survey of Namibia, Windhoek, **2**, 13.69–13.136.

Hyodo, H. & Dunlop, D. J. 1993. Effect of anisotropy on the paleomagnetic contact test for a Grenville Dike. *Journal of Geophysical Research*, **98**, 7997–8017.

Jaffey, A. H., Flynn, K. F., Glendenin, L. E., Bentley, W. C. & Essling, A. M. 1971. Precision measurements of half-lives and specific activities of ^{235}U and ^{238}U. *Physics Review*, **C4**, 1889–1906.

Johansson, Å., Gee, D. G., Larionov, A. N., Ohta, Y. & Tebenkov, A. M. 2005. Grenvillian and Caledonian evolution of eastern Svalbard– a tale of two orogenies. *Terra Nova*, **17**, 317–325.

Johnson, S. P., Rivers, T. & De Waele, B. 2005. A review of the Mesoproterozoic to early Palaeozoic magmatic and tectonothermal history of south–central Africa: implications for Rodinia and Gondwana. *Journal of the Geological Society of London*, **162**, 433–450.

Key, R. M., Liyungu, A. K., Njamu, F. M., Somwe, V., Banda, J., Mosley, P. N. & Armstrong, R. A. 2001. The western arm of the Lufilian Arc in NW Zambia and its potential for copper mineralization. *Journal of African Earth Sciences*, **33**, 503–528.

Kirschvink, J. L. 1980. The least-squares line and plane and the analysis of paleomagnetic data. *Geophysical Journal of the Royal Astronomical Society*, **62**, 699–718.

Kirschvink, J. L., Kopp, R. E., Raub, T. D., Baumgartner, C. T. & Holt, J. W. 2008. Rapid, precise, and

high-sensitivity acquisition of paleomagnetic and rock-magnetic data: development of a low-noise automatic sample changing system for superconducting rock magnetometers. *Geochemistry Geophysics Geosystems*, **9**, http://doi.org/10.1029/2007GC001856

KOKONYANGI, J. W., KAMPUNZU, A. B., ARMSTRONG, R., YOSHIDA, M., OKUDAIRA, T., ARIMA, M. & NGULUBE, D. A. 2006. The Mesoproterozoic Kibaride belt (Katanga, SE D.R. Congo). *Journal of African Earth Sciences*, **46**, 1–35.

KRÖNER, A. & CORDANI, U. G. 2003. African, southern Indian and South American cratons were not part of the Rodinia supercontinent: evidence from field relationships and geochronology. *Tectonophysics*, **375**, 325–352.

LI, Z. X., BOGDANOVA, S. V. *ET AL.* 2008. Assembly, configuration, and break-up history of Rodinia: a synthesis. *Precambrian Research*, **160**, 179–210.

LOVE, J. J. 2000. Statistical assessment of preferred transitional VGP longitudes based on paleomagnetic lava data. *Geophysical Journal International*, **140**, 211–221.

LUDWIG, K. R. 2003. *ISOPLOT: a Plotting and Regression Program for Radiogenic Isotope Data, Version Ex/3.00*. Berkeley Geochronology Center, Berkeley, CA, Special Publications, **4**.

MACHADO, N., SCHRANK, A., ABREU, F. R., KNAUER, L. G. & ALMEIDA-ABREU, P. A. 1989. Resultados preliminares da geocronologia U–Pb na Serra do Espinhaço Meridional. *Anais V Simpósio de Geologia de Minas Gerais, Boletim da Sociedade Brasileira Geologia-Núcleo Minas Gerais*, **10**, 171–174.

MCELHINNY, M. W., POWELL, C. McA. & PISAREVSKY, S. A. 2003. Paleozoic terranes of eastern Australia and the drift history of Gondwana. *Tectonophysics*, **362**, 41–65.

MCFADDEN, P. L. & MCELHINNY, M. W. 1990. Classification of the reversal test in palaeomagnetism. *Geophysical Journal International*, **103**, 725–729.

MEERT, J. G. & TORSVIK, T. H. 2003. The making and unmaking of a supercontinent: Rodinia revisited. *Tectonophysics*, **375**, 261–288.

MEERT, J. G. & VAN DER VOO, R. 1996. Paleomagnetic and $^{40}Ar/^{39}Ar$ study of the Sinyai dolerite, Kenya: implications for Gondwana assembly. *Journal of Geology*, **104**, 131–142.

MEERT, J. G., VAN DER VOO, R., POWELL, C. McA., LI, Z.-X., MCELHINNY, M. W., CHEN, Z. & SYMONS, D. T. A. 1993. A plate-tectonic speed limit? *Nature*, **363**, 216–217.

MEERT, J. G., HARGRAVES, R. B., VAN DER VOO, R., HALL, C. M. & HALLIDAY, A. N. 1994. Paleomagnetic and $^{40}Ar/^{39}Ar$ studies of late Kibaran intrusives in Burundi, East Africa: implications for Late Proterozoic supercontinents. *Journal of Geology*, **102**, 621–637.

PAVLOV, V. & GALLET, Y. 2010. Variations in geomagnetic reversal frequency during the Earth's middle age. *Geochemistry Geophysics Geosystems*, **11**, http://doi.org/10.1029/2009GC002583

PEDROSA-SOARES, A. C. & ALKMIM, F. F. 2011. How many rifting events preceded the development of the Araçuaí–West Congo orogen? *Geonomos*, **19**, 244–251.

PENG, P., BLEEKER, W., ERNST, R. E., SÖDERLUND, U. & MCNICOLL, V. 2011. U–Pb baddeleyite ages, distribution and geochemistry of 925 Ma mafic dykes and 900 Ma sills in the North China craton: evidence for a Neoproterozoic mantle plume. *Lithos*, **127**, 210–221.

PIPER, J. D. A. 2007. The Neoproterozoic supercontinent Palaeopangaea. *Gondwana Research*, **12**, 202–227.

PISAREVSKY, S. A. & BYLUND, G. 2006. Palaeomagnetism of 935 Ma mafic dykes in southern Sweden and implications for the Sveconorwegian Loop. *Geophysical Journal International*, **166**, 1095–1104.

PISAREVSKY, S. A., WINGATE, M. T. D., POWELL, C. McA., JOHNSON, S. & EVANS, D. A. D. 2003. Models of Rodinia assembly and fragmentation. *In*: YOSHIDA, M., WINDLEY, B. F. & DASGUPTA, S. (eds) *Proterozoic East Gondwana: Supercontinent Assembly and Breakup*. Geological Society, London, Special Publications, **206**, 35–55.

POIDEVIN, J.-L. 2007. Stratigraphie isotopique du strontium et datation des formations carbonatées et glaciogéniques néoprotérozoiques du Nord et de l'Ouest du craton du Congo. *Comptes Rendus Geoscience*, **339**, 259–273.

POWELL, C. McA., LI, Z. X., MCELHINNY, M. W., MEERT, J. G. & PARK, J. K. 1993. Paleomagnetic constraints on timing of the Neoproterozoic breakup of Rodinia and the Cambrian formation of Gondwana. *Geology*, **21**, 889–892.

RAPOSO, M. I. B. & BERQUÓ, T. S. 2008. Tectonic fabric revealed by AARM of the Proterozoic mafic dike swarm in the Salvador city (Bahia State): São Francisco Craton, NE Brazil. *Physics of the Earth and Planetary Interiors*, **167**, 179–194.

RENNE, P. R., ONSTOTT, T. C., D'AGRELLA-FILHO, M. S., PACCA, I. G. & TEIXEIRA, W. 1990. $^{40}Ar/^{39}Ar$ dating of 1.0–1.1 Ga magnetizations from the São Francisco and Kalahari cratons: tectonic implications for Pan-African and Brasiliano mobile belts. *Earth and Planetary Science Letters*, **101**, 349–366.

SCHÄRER, U., WILMART, E. & DUCHESNE, J.-C. 1996. The short duration and anorogenic character of anorthosite magmatism: U–Pb dating of the Rogaland complex, Norway. *Earth and Planetary Science Letters*, **139**, 335–350.

SCHERSTÉN, A., ÅREBÄCK, H., CORNELL, D., HOSKIN, P., ÅBERG, A. & ARMSTRONG, R. 2000. Dating mafic-ultramafic intrusions by ion-microprobing contact-melt zircon: examples from SW Sweden. *Contributions to Mineralogy and Petrology*, **139**, 115–125.

SMIRNOV, A. V., TARDUNO, J. A. & EVANS, D. A. D. 2011. Evolving core conditions *c.* 2 billion years ago detected by paleosecular variation. *Physics of the Earth and Planetary Interiors*, **187**, 225–231.

SÖDERLUND, U. & JOHANSSON, L. 2002. A simple way to extract baddeleyite (ZrO2). *Geochemistry, Geophysics, Geosystems*, **3**, 1–7.

STACEY, J. S. & KRAMERS, J. D. 1975. Approximation of terrestrial lead isotope evolution by a two-stage model. *Earth and Planetary Science Letters*, **26**, 207–221.

STEARN, J. E. F. & PIPER, J. D. A. 1984. Palaeomagnetism of the Sveconorwegian mobile belt of the Fennoscandian Shield. *Precambrian Research*, **23**, 201–246.

Su, W.-B., Li, H.-K., Xu, L., Jia, S.-H., Geng, J.-Z., Zhou, H.-Y., Wang, Z.-H. & Pu, H.-Y. 2012. Luoyu and Ruyang Group at the South Margin of the North China Craton (NCC) Should Belong in the Mesoproterozoic Changchengian System: direct constraints from the LA-MC-ICPMS U–Pb Age of the Tuffite in the Luoyukou Formation, Ruzhou, Henan, China. *Geological Survey and Research*, **35**, 96–108[in Chinese with English abstract].

Swanson-Hysell, N. L., Maloof, A. C., Weiss, B. P. & Evans, D. A. D. 2009. No asymmetry in geomagnetic reversals recorded by 1.1-billion-year-old Keweenawan basalts. *Nature Geoscience*, **2**, 713–717.

Tack, L., Wingate, M. T. D., Liégeois, J.-P., Fernandez-Alonso, M. & Deblond, A. 2001. Early Neoproterozoic magmatism (1000–910 Ma) of the Zadinian and Mayumbian Groups (Bas-Congo): onset of Rodinia rifting at the western edge of the Congo craton. *Precambrian Research*, **110**, 277–306.

Trompette, R. 1994. *Geology of Western Gondwana (2000–500 Ma). Pan-African–Brasiliano Aggregation of South America and Africa*. Balkema, Rotterdam.

Ueno, H., Irving, E. & McNutt, R. H. 1975. Paleomagnetism of the Whitestone anorthosite and diorite, the Grenville polar track, and relative motions of the Laurentian and Baltic Shields. *Canadian Journal of Earth Sciences*, **12**, 209–226.

Verwey, E. J. W. 1939. Electronic conduction of magnetite (Fe_3O_4) and its transition point at low-temperature. *Nature*, **44**, 327–328.

Walderhaug, H. J., Torsvik, T. H. & Halvorsen, E. 2007. The Egersund dykes (SW Norway): a robust Early Ediacaran (Vendian) palaeomagnetic pole from Baltica. *Geophysical Journal International*, **168**, 935–948.

Warnock, A. C., Kodama, K. P. & Zeitler, P. K. 2000. Using thermochronometry and low-temperature demagnetization to accurately date Precambrian paleomagnetic poles. *Journal of Geophysical Research*, **105**, 19435–19453.

Watt, G. R. & Thrane, K. 2001. Early Neoproterozoic events in East Greenland. *Precambrian Research*, **110**, 165–184.

Weil, A. B., Van der Voo, R., Mac Niocaill, C. & Meert, J. G. 1998. The Proterozoic supercontinent Rodinia: paleomagnetically derived reconstructions for 1100 to 800 Ma. *Earth and Planetary Science Letters*, **154**, 13–24.

Wingate, M. T. D. & Giddings, J. W. 2000. Age and palaeomagnetism of the Mundine Well dyke swarm, Western Australia: implications for an Australia–Laurentia connection at 755 Ma. *Precambrian Research*, **100**, 335–357.

Wingate, M. T. D., Pisarevsky, S. A. & Evans, D. A. D. 2002. Rodinia connections between Australia and Laurentia: no SWEAT, no AUSWUS? *Terra Nova*, **14**, 121–128.

Yamasaki, T. & Stephenson, R. 2009. Potential role of strain hardening in the cessation of rifting at constant tectonic force. *Journal of Geodynamics*, **47**, 47–62.

Zhang, S., Li, Z.-X. & Wu, H. 2006. New Precambrian palaeomagnetic constraints on the position of the North China Block in Rodinia. *Precambrian Research*, **144**, 213–238.